HHS Public Access

Author manuscript

Nat Immunol. Author manuscript; available in PMC 2021 January 13.

Published in final edited form as:

Nat Immunol. 2020 September ; 21(9): 1022–1033. doi:10.1038/s41590-020-0725-2.

Impaired mitochondrial oxidative phosphorylation limits the self-renewal of T cells exposed to persistent antigen

Santosha A. Vardhana[1,2,4], **Madeline A. Hwee**[1,2], **Mirela Berisa**[3], **Daniel K. Wells**[4], **Kathryn E. Yost**[5], **Bryan King**[1,2], **Melody Smith**[6], **Pamela S. Herrera**[6,7], **Howard Y. Chang**[5,8], **Ansuman T. Satpathy**[4,9], **Marcel R.M. van den Brink**[6], **Justin R. Cross**[3], **Craig B. Thompson**[1,2,*]

[1]Cancer Biology and Genetics Program, Memorial Sloan Kettering Cancer Center, New York, New York, USA

[2]Center for Epigenetics Research, Memorial Sloan Kettering Cancer Center, New York, New York, USA

[3]The Donald B. and Catherine C. Marron Cancer Metabolism Center, Memorial Sloan Kettering Cancer Center, New York, New York, USA

[4]Parker Institute for Cancer Immunotherapy, San Francisco, CA, USA

[5]Center for Personal Dynamic Regulomes, Stanford University School of Medicine, Stanford, CA, USA

[6]Department of Medicine and Immunology Program, Memorial Sloan Kettering Cancer Center, New York, New York, USA

[7]Weill Cornell Medical College, New York, New York, USA

[8]Howard Hughes Medical Institute, Stanford University School of Medicine, Stanford, CA 94305

[9]Department of Pathology, Stanford University School of Medicine, Stanford, CA, USA

Abstract

The majority of tumor-infiltrating T cells exhibit a terminally exhausted phenotype, marked by a loss of self-renewal capacity. How repetitive antigenic stimulation impairs T cell self-renewal remains poorly defined. Here we show that persistent antigenic stimulation impaired ADP-coupled oxidative phosphorylation. The resultant bioenergetic compromise blocked proliferation by limiting nucleotide triphosphate synthesis. Inhibition of mitochondrial oxidative phosphorylation

*Correspondence: thompsonc@mskcc.org.

Author Contributions

S.A.V. and C.B.T. conceived the study. S.A.V. performed all experiments with assistance from M.A.H. M.B and J.R.C. assisted with LC-MS, extracellular flux, and nutrient consumption experiments. D.K.W., B.K., A.T.S., H.Y.C, and K.E.Y. assisted with analysis of RNA-sequencing data. M.S., P.S.H., and M.vdB. assisted with CAR-T cell experiments. C.B.T. provided additional work in conception and study guidance. S.A.V. and C.B.T. wrote the manuscript.

Additional Information

Supplementary information is available for this paper. Reprints and permissions information is available at www.nature.com/reprints. Further information and requests for reagents may be directed to, and will be fulfilled by, the corresponding authors, Craig B. Thompson (thompsonc@mskcc.org).

in activated T cells was sufficient to suppress proliferation and upregulate genes linked to T cell exhaustion. Conversely, prevention of mitochondrial oxidative stress during chronic T cell stimulation allowed sustained T cell proliferation and induced genes associated with stem-like progenitor T cells. As a result, antioxidant treatment enhanced the anti-tumor efficacy of chronically stimulated T cells. These data reveal that loss of ATP production through oxidative phosphorylation limits T cell proliferation and effector function during chronic antigenic stimulation. Furthermore, treatments that maintain redox balance promote T cell self-renewal and enhance anti-tumor immunity.

Keywords

T cell; metabolism; immunotherapy; checkpoint blockade; oxidative stress; Tcf7; exhaustion; terminal exhaustion; antioxidant; glucose

Introduction

Suppression of endogenous anti-tumor immune responses is frequently required for tumor initiation and growth[1]. Intratumoral T cell failure often occurs despite the ability to recognize cancer-specific antigens, due to a series of functional defects known collectively as T cell “exhaustion.” T cell exhaustion is defined by loss of proliferative capacity, decreased production of cytotoxic effector molecules, and upregulation of inhibitory immunoreceptors such as Programmed Death-1 (PD-1) and cytotoxic T-lymphocyte-associated protein 4 (CTLA-4)[2]. Enhancing T cell function via immune checkpoint blockade or ectopic expression of chimeric antigen receptors (CARs) has shown promise for treating cancer[3]; unfortunately, the majority of patients still fail to durably respond to immune-based therapy.

How immune checkpoint blockade reactivates endogenous immune responses remains the subject of some controversy. Intratumoral T cells from patients with durable response to immunotherapy express genes associated with memory and self-renewal[4, 5, 6], whereas T cells from patients who fail to respond to immunotherapy acquire a “terminally exhausted” phenotype marked by impaired proliferation[7, 8]. Loss of proliferative capacity ultimately limits the clinical activity of checkpoint inhibitors and underscores a need to identify strategies to restore or maintain a self-renewal program in exhausted T cells.

Our laboratory previously demonstrated that T cell proliferation requires activation-induced glucose uptake as well as a rewiring of glucose metabolism to support macromolecular synthesis required for proliferation[9], and that inhibitory immunoreceptors such as PD-1 and CTLA-4 act in part by reducing activation-induced glucose uptake[10]. T cells extracted from tumors show signs of metabolic dysfunction[11, 12, 13]. However, whether altered metabolism is responsible for either the functional defects or altered gene expression observed in exhausted T cells remains unknown.

Here we show that impaired mitochondrial ATP production during chronic antigenic stimulation limits T cell self-renewal capacity and promotes terminal differentiation. Despite exhibiting a glycolytic phenotype, terminally exhausted T cells are unable to proliferate.

Functional interrogation of T cells during chronic stimulation revealed impairment of ADP-coupled oxidative phosphorylation. The uncoupling of electron transport from mitochondrial reduction of NAD^+ to NADH resulted in generation of reactive oxygen species (ROS) rather than maintenance of cellular nucleotide triphosphate levels. Direct inhibition of mitochondrial oxidative phosphorylation suppressed proliferation as well as expression of genes associated with T cell self-renewal while activating genes associated with terminal differentiation. Finally, preventing persistent antigen-driven accumulation of mitochondrial ROS with antioxidants restored T cell proliferation, effector function, and memory cell-associated gene expression and enhanced anti-tumor T cell immunity *in vitro* and *in vivo*. These data establish that chronic stimulation-dependent mitochondrial dysfunction is a major factor in limiting anti-tumor immunity and highlights the importance of metabolic cues in directing T cell fate decisions within the tumor microenvironment.

Results

T cell exhaustion is driven by persistent antigen

To better understand how changes in cellular metabolism might contribute to the development of T cell exhaustion, we developed an *in vitro* system in which activated T cells were expanded in the absence (“acute”) or presence (“chronic”) of persistent antigenic stimulation in the form of either tumors with or without specific antigen (OVA) or anti-CD3-mediated stimulation of the T cell antigen receptor (TCR). Cells were passaged every 2 days with or without persistent stimulation, and both acutely and chronically stimulated T-cells were briefly re-stimulated for 6 h prior to harvest. Chronically stimulated T cells generated using these protocols failed to produce effector cytokines and upregulated expression of inhibitory immunoreceptors associated with exhausted T cells (Fig. 1a and Extended Data 1a–c). Moreover, chronic stimulation *in vitro* was sufficient to activate a transcriptional signature associated with T cell exhaustion. RNA-sequencing revealed that T cells that were chronically stimulated for 8 days were highly enriched for genes upregulated in tumor-infiltrating exhausted T cells from both mouse models and patients as well as T cells isolated from mice with chronic LCMV infections, but not significantly for genes upregulated in anergic T cells (Fig. 1b and Extended Data 1e)[6, 14, 15, 16]. Accordingly, in sharp contrast to activated OT-I T cells expanded without persistent TCR stimulation, chronically stimulated T cells were unable to kill cognate antigen-expressing tumor cells *in vitro*, nor were they able to suppress tumor growth following adoptive transfer *in vivo* (Fig. 1c and Extended Data 1f). Collectively, these results establish that chronic *in vitro* T cell stimulation can recapitulate the hallmarks of *in vivo* T cell exhaustion and offered the opportunity to evaluate the contribution of altered metabolic behavior to the development of this process.

Enhanced glycolysis is a hallmark of terminally exhausted T cells

During conventional immune responses, activated T cells increase glucose uptake[9] as well as the fraction of glucose excreted as lactate, a phenomenon known as “aerobic glycolysis”[17, 18]. We found that T cells expanded in the presence of persistent antigen maintained higher rates of both glucose transporter expression and glucose uptake than activated OT-I T cells expanded in the absence of repetitive antigen exposure (Fig. 1d and Extended Data 1d). They also exhibited higher rates of lactate excretion that was almost

entirely glucose-derived (Fig. 1e and Extended Data 1g–h). Extracellular flux analysis of the expanded T cells demonstrated that chronically stimulated T cells maintained increased rates of extracellular acidification that were dependent on available glucose and inhibited by 2-deoxy-D-glucose, which blocks the conversion of glucose to glucose-6-phosphate (Extended Data 2a). The extracellular acidification rate of chronically stimulated T cells could only be marginally increased upon re-stimulation or treatment with rotenone and antimycin A, suggesting that chronically stimulated T cells have minimal glycolytic reserve (Fig. 1f and Extended Data 2b). In proliferating cells, activation of aerobic glycolysis reflects the need to balance glucose uptake with the production of anabolic precursors as byproducts of glycolytic and TCA cycle activity[18]. In T cells, co-stimulation of the TCR and CD28 receptors synergize to induce aerobic glycolysis in support of both proliferation and effector function[9]. It was therefore puzzling that, despite high rates of glycolysis, chronically stimulated T cells displayed a progressively reduced ability to proliferate as they were passaged (Fig. 1g and Extended Data 2c). The decreased accumulation of chronically stimulated T cells over time was primarily attributable to a loss in proliferative capacity rather than a decrease in cell viability, which was only slightly decreased after eight days in culture (Extended Data 2d–e).

While loss of proliferative capacity is a hallmark of a subset of exhausted T cells with a "terminally exhausted" phenotype[6, 8], it has not been reported that such cells display enhanced glycolysis compared to proliferating T cells or effector cells. To examine this issue, we analyzed single-cell transcriptomes from intratumoral T cells isolated from both mice bearing B16 melanoma tumors, as well as patients who were treated with immune checkpoint inhibition (ICI) in independent clinical studies[6, 8, 19]. We found that a glycolytic gene signature was increased in terminally exhausted T cell subsets as compared to either progenitor-like exhausted or conventional effector T cells isolated from human melanomas, basal cell carcinomas, and squamous cell carcinomas (Fig. 1h and Extended Data 2f). Similarly, glycolytic genes were significantly enriched in terminally exhausted T cells from B16 melanoma-bearing mice as compared to progenitor exhausted T cells (Extended Data 2g). Consistent with these findings, we observed a significant inverse correlation between expression of glycolytic genes and expression of *TCF7*, which is essential for intratumoral T cell self-renewal[4], but observed no such correlation between tricarboxylic citric acid cycle genes and *TCF7* expression in basal and squamous cell carcinomas (Extended Data 2h).

Given that terminally exhausted T cells were enriched in glycolytic genes, we next asked whether chronically stimulated T cells *in vitro* exhibited a terminally exhausted phenotype. T cells expanded in the presence of persistent antigen were significantly enriched for genes that distinguished terminally exhausted T cells from stem-like progenitor exhausted T cells (Fig. 1i and Extended Data 2i) and upregulated the exhaustion-associated transcription factor TOX, while decreasing expression of the transcription factor TCF-1, which marks progenitor-like exhausted cells (Fig. 1j)[4, 7, 20, 21, 22]. Additionally, T cells expanded in the presence of persistent antigen were unable to produce effector cytokines, even when PD-1–PD-L1 interactions were blocked during priming (Extended Data 2j) and were unable to recover functionally after antigen withdrawal (Extended Data 2k). This functional incapacitation is similar to that of terminally exhausted T cells, which exhibit a phenotype that cannot be reversed by ICI or antigen withdrawal.

Chronic T cell stimulation leads to loss of mitochondrial function

Even with high rates of glycolysis, most cells require intact mitochondrial function to proliferate[23]. We therefore asked whether the highly glycolytic phenotype exhibited by chronically stimulated T cells might reflect decreased mitochondrial capacity. T cell activation increases mitochondrial oxygen consumption by stimulating inositol-3-phosphate-dependent electron transport chain activity[24, 25]. We found that while, similar to acutely activated T cells, mitochondrial oxygen consumption increased early during chronic stimulation, it progressively declined as the cells were passaged, such that mitochondrial oxygen consumption was significantly decreased relative to acutely stimulated cells by day 8 and nearly absent by day 14 (Fig. 2a). In contrast to activated T cells expanded in the absence of persistent antigen, T cells that had been chronically stimulated for eight days were unable to increase oxygen consumption in response to anti-CD3 (Fig. 2b). In addition, steady-state concentrations of TCA cycle metabolites were reduced in chronically stimulated T cells as compared to acutely stimulated T cells (Extended Data 3a). The inability to activate mitochondrial oxidative phosphorylation in response to persistent antigenic stimulation correlated with an increasing reliance on glycolysis for ATP production and markedly reduced glucose-dependent spare respiratory capacity, suggesting a defect in the ability of chronically stimulated T cells to oxidize glucose to maintain cellular bioenergetics (Fig. 2c and Extended Data 3b).

To confirm the above findings, we traced the fate of uniformly ^{13}C-labeled glucose ([U-^{13}C] glucose) in acutely and chronically stimulated T cells (Fig. 2d). Condensation of glucose-derived acetyl-CoA and oxaloacetate to generate citrate was largely unaffected, suggesting that despite high rates of aerobic glycolysis, delivery of glucose-derived acetyl-CoA to the TCA cycle was unimpaired (Fig. 2e). However, chronic T cell stimulation significantly decreased the fraction of downstream TCA cycle metabolites derived from glucose (Fig. 2e). The defect in mitochondrial oxidation of carbon substrates was not unique to glucose, as isotope tracing of [U-^{13}C] palmitate demonstrated markedly reduced contribution of palmitate to all TCA cycle metabolites, indicating an impairment in mitochondrial beta-oxidation (Extended Data 3c–d). Taken together, these findings suggest a generalized defect in the mitochondrial oxidative capacity of chronically stimulated T cells.

Persistent antigen limits T cell nucleotide triphosphate synthesis

We next asked how defective mitochondrial oxidation might contribute to terminal T cell exhaustion during persistent antigen stimulation. Cellular proliferation depends on the net production of proteins, lipids, and nucleic acids[23, 26, 27, 28]. Chronically stimulated T cells demonstrated both intact glucose-dependent citrate production as well as an increased contribution of glucose to lipid biosynthesis, suggesting that lipid synthesis is not limiting for T cell proliferation during chronic stimulation (Fig. 2e,f). Furthermore, supplementation of acetate, which offers an independent source of acetyl-CoA for lipid synthesis[28], did not restore proliferation in chronically stimulated T cells (Extended Data 3e).

A second role for the TCA cycle in proliferating cells is to generate precursors that support nucleotide biosynthesis[23, 27]. An unbiased LC-MS-based assessment of steady-state metabolites in acutely and chronically stimulated T cells found that both purine and

pyrimidine precursors as well as monophosphorylated purines and pyrimidines were increased in T cells expanded in the presence of antigen (Extended Data 3f). As we were unable to demonstrate a reduced ability to produce lipid and nucleotide precursors, we next asked whether nucleotide triphosphate pools might be compromised as a result of the reduced oxidative phosphorylation exhibited by T cells expanded in the presence of persistent antigen. LC-MS analysis revealed a decrease in all nucleotide triphosphates and increases in nucleosides and/or nucleotide monophosphates, such that the ratio of nucleotide triphosphates to their corresponding nucleotide monophosphates or nucleosides were all significantly decreased (Fig. 2g–h). As the iterative phosphorylation of nucleotides by nucleotide diphosphate kinase requires ATP, we assessed whether the ATP/AMP ratio was decreased in chronically stimulated T cells and found that this ratio progressively decreased over the course of chronic T cell stimulation (Fig. 2i). The synthesis of DNA and protein are highly dependent on a continuous supply of ATP and this reduction is consistent with the progressive loss of the ability to proliferate or produce cytokine in T cells exposed to persistent antigen.

Oxidative stress promotes terminal T cell differentiation

Our observation that mitochondrial insufficiency develops when activated T cells are expanded during persistent antigen exposure are consistent with reports suggesting that tumor-infiltrating lymphocytes exhibit mitochondrial dysfunction[11, 13, 29]. The defective oxidative phosphorylation we observed during chronic antigenic stimulation was not due to impaired mitochondrial biogenesis or mitochondrial protein expression, which were in fact increased during chronic stimulation (Fig. 3a,b). Rather, we observed an increase in the $NADH/NAD^+$ ratio during chronic T cell stimulation (Fig. 3c). Given the observed decrease in ATP/AMP ratios, this indicated uncoupling of mitochondrial NADH generation from oxidative phosphorylation and ATP synthesis.

To test the effect of lowering the redox load of chronically stimulated T cells, we overexpressed water-forming NADH oxidases from *Lactobacillus brevis* (LbNOX) in both the cytoplasm and mitochondria of chronically stimulated T cells (Extended Data 4a). Complementation of electron transport chain (ETC) activity by overexpressing LbNOX has been shown to decrease the $NADH/NAD^+$ ratio and decrease redox stress in cells with impaired mitochondrial function[30]. We found that LbNOX overexpression reduced redox stress in T cells expanded in the presence of persistent antigen (Extended Data 4b) and partially restored the proliferative capacity of chronically stimulated T cells, suggesting the increased reductive stress that accompanies persistent antigenic exposure contributed to the impaired oxidative phosphorylation we had observed (Extended Data 4c).

One way that increased reductive stress can contribute to uncoupling of oxidative phosphorylation is through the generation of reactive oxygen species (ROS). ROS can directly interfere with mitochondrial ATP synthesis by inactivating iron-sulfur cluster-containing proteins within the ETC. We therefore hypothesized that the decreased mitochondrial ATP synthesis in the face of an increased $NADH/NAD^+$ ratio observed in chronically stimulated T cells might be due to ROS-mediated inactivation of mitochondrial electron transport. To test this possibility, we examined ROS generation in T cells

proliferating in the presence or absence of persistent antigen exposure. In comparison to activated T cells expanded in the absence of chronic TCR engagement, T cells exposed to chronic antigen accumulated high levels of both cellular and mitochondrial ROS, resulting in increased levels of lipid peroxidation (Fig. 3d and Extended Data 4d).

Mitochondrial uncoupling suppresses T cell self-renewal

Free radicals such as superoxides generated within the mitochondria are rapidly converted to hydrogen peroxide (H_2O_2) via superoxide dismutase. H_2O_2 reacts with metal ions such as iron present within multiple components of the ETC as well as several enzymes within the tricarboxylic acid cycle and can rapidly lead to their inactivation[31]. To test whether disruption of iron sulfur cluster-containing complexes involved in electron transport could reproduce the phenotype of exhausted T cells, we treated activated T cells with inhibitors of complexes I (rotenone) and V (oligomycin) of the electron transport chain or cobalt chloride ($CoCl_2$), which inactivates iron-sulfur cluster-containing proteins, in the absence of further antigenic stimulation[32]. Cells were treated after 2 days of initial stimulation given the known requirement of mitochondrial oxidative phosphorylation for T cell activation[33]. All treatments increased ROS, reduced ATP/AMP ratios, and reduced subsequent T cell proliferation, suggesting that impairing oxidative phosphorylation alone is sufficient to cause bioenergetic compromise and impair growth (Fig. 3e–f and Extended Data 4e). In addition to reducing T cell proliferation, all three inhibitors reduced TCF-1 expression and activated TOX expression (Fig. 3g). We confirmed loss of expression of self-renewal genes by quantitative PCR (Extended Data 4f).

To determine whether ROS accumulation is also a hallmark of exhausted T cells in patients, we analyzed single-cell RNA-seq data from T cells isolated from patients with melanoma, basal cell carcinoma, and squamous cell carcinoma from independent data sets[6, 19]. We found that terminally exhausted T cells were significantly enriched in genes associated with response to oxidative stress in both patient data sets (Fig. 3h and Extended Data 4g). Notably, in patients in whom both single-cell RNA sequencing and TCR sequencing were performed, we observed a progressive increase in oxidative stress genes with increasing clone size only in exhausted T cells but not in memory T cells (Extended Data 4h). Finally, we noted an inverse relationship between expression of oxidative stress response genes and *TCF7* in exhausted T cells from patient tumors (Fig. 3i and Extended Data 4i). Collectively, these results demonstrate that oxidative stress is a consequence of chronic antigen-driven mitochondrial dysfunction and is sufficient to impair T cell proliferation and self-renewal.

Antigen-driven ROS is associated with sustained NFAT activity

We next asked how mitochondrial dysfunction might activate the exhaustion-associated gene expression program. Nuclear translocation of NFAT is known to require complex III-dependent mitochondrial ROS production[24]; furthermore, NFAT is known to bind to the *TOX* promoter and activate *TOX* transcription[34], and constitutively active NFAT has been shown to activate many aspects of the exhaustion-associated transcriptional program[35]. We confirmed strong enrichment of NFAT-binding motifs at sites with increased chromatin accessibility early during the development of intratumoral T cell dysfunction *in vivo* (Extended Data 5a)[15]. Nuclear NFAT translocation requires calcium-dependent calcineurin

phosphatase activity, suggesting that sustained intracellular calcium elevation might promote both mitochondrial ROS and downstream NFAT activation. Consistent with this hypothesis, we found that chronically stimulated T cells exhibited higher concentrations of intracellular calcium both at baseline and in response to monomeric T cell receptor stimulation, whereas activated T cells expanded in the presence of interleukin 2 (IL-2) increased intracellular calcium levels only in response to TCR crosslinking (Extended Data 5b). As a result, RNA-sequencing of activated T cells expanded in the presence of persistent antigen demonstrated increased expression of NFAT target genes as compared to activated T cells expanded in the presence of IL-2 alone (Extended Data 5c). To confirm that elevated NFAT activity was associated with oxidative stress and terminal T cell exhaustion in patient samples, we analyzed single-cell RNA sequencing data from intratumoral T cells isolated from melanoma patients. We found that expression of NFAT target genes correlated highly with expression of genes related to oxidative stress; as a result, an NFAT target gene signature was highly enriched within terminally exhausted T cells (Extended Data 5d–e). Taken together, these findings suggest that heightened NFAT activity in response to calcium-driven mitochondrial ROS contributes to development of T cell exhaustion.

N-acetylcysteine reverses antigen-driven T cell metabolic defects

Given that ROS accumulation restricts both proliferation and expression of genes required for self-renewal in chronically stimulated T cells, we asked whether neutralizing intracellular ROS could restore T cell self-renewal. Lymphocyte function in standard culture media can be improved by the addition of β-mercaptoethanol (β-ME)[36], which prevents the oxidation of free sulfhydryl residues and acts as a buffer against the generation of free radicals. Supplementation of β-ME could partially restore the proliferation and cytokine production of chronically stimulated T cells (Fig. 4a–b). However, even in the presence of excess β-ME, T cells cultured in the presence of persistent antigen displayed residual ROS accumulation as measured by CM-H_2DCFDA fluorescence (Extended Date 5f).

Glutathione serves an essential role in cellular redox control by neutralizing intracellular ROS and detoxifying metabolites produced by free radicals. Endogenous glutathione synthesis is required to prevent ROS-dependent toxicity during T cell activation[37]. We therefore hypothesized that chronic stimulation-dependent ROS accumulation might increase the cellular dependence on glutathione-antioxidant defense. To investigate this hypothesis, we cultured T cells in medium containing either standard tissue culture concentrations (100 μM) or ten-fold reductions (10 μM) in the concentrations of extracellular cysteine to limit endogenous glutathione synthesis. Consistent with a requirement for *de novo* glutathione for T cell activation and proliferation, acutely stimulated T cells were partially sensitive to reductions in available cysteine (31.6% reduction in proliferation) (Fig. 4c, left). However, T cells cultured in the presence of persistent antigen had an even greater reduction (71.1%) in their proliferation (Fig. 4c, right) and exhibited increased expression of PD-1 (Fig 4d). To confirm the requirement of glutathione for T cell self-renewal, we blocked endogenous glutathione synthesis using buthionine sulfoximine (BSO), an inhibitor of gamma-glutamylcysteine synthetase, or increased endogenous glutathione consumption using the oxidizing agent diamide. Acutely stimulated T cells exhibited diminished proliferation as well as decreased expression of

TCF-1 and increased expression of TOX in the presence of either BSO or diamide (Fig. 4f and Extended Data 5g). Chronically stimulated T cells were unable to survive in the absence of *de novo* glutathione synthesis (Extended Data 5h). Finally, using two-dimensional killing assays, we found that the ability of T cells to kill tumor cells was particularly sensitive to cysteine withdrawal (Fig. 4e). Thus, chronic stimulation-driven mitochondrial dysfunction and ROS accumulation increases sensitivity to glutathione depletion.

One mechanism to increase cellular uptake of cysteine is to add a cell-permeant form of cysteine to the culture medium. We therefore assessed whether supplementing T cells with N-acetylcysteine (N-AC, 10 mM) could restore metabolic T cell function during chronic stimulation. N-AC supplementation increased glutathione synthesis, suggesting that cysteine availability is limiting for the maintenance of glutathione pools in chronically stimulated T cells (Fig. 5a and Extended Data 6a). As a result, N-AC decreased intracellular ROS and increased the oxygen consumption rate of chronically stimulated T cells, suggesting that increasing intracellular cysteine levels can help maintain ADP-coupled oxidative phosphorylation during chronic T cell stimulation (Fig. 5b–c). Moreover, N-AC increased the fractional labeling of TCA cycle intermediates by [U-^{13}C] glucose, indicating increased mitochondrial oxidation of glucose-derived citrate (Fig. 5d). As a result, N-AC supplementation rescued the ATP/AMP ratio and ATP production in chronically stimulated T cells, enabling restoration of nucleotide triphosphate levels while reducing the levels of nucleosides and nucleotide monophosphates (Fig. 5e–g and Extended Data 6b).

N-acetylcysteine restores self-renewal in exhausted T cells

N-AC restored the proliferation of chronically stimulated T cells (Fig. 6a). This rescue was abrogated under hypoxic conditions (Extended Data 7a), suggesting that the ability of N-AC to restore T cell self-renewal depends on oxygen-dependent, ETC-mediated ATP synthesis. To determine whether the restoration of proliferation by N-AC was accompanied by a change in gene expression, we performed RNA-sequencing on acutely and chronically stimulated T cells in the presence or absence of N-AC. Principle component analysis demonstrated that T cells chronically stimulated in the presence of N-AC clustered separately from both acutely and chronically stimulated cells (Fig. 6b). Among the genes most strongly contributing to variance between N-AC treated and untreated chronically stimulated T cells were genes encoding memory-associated transcription factors such as *Tcf7*, *Pou6f1*, and *Pou2af1*, as well as genes associated with terminal exhaustion, such as *Mt1*, *Mt2*, *Il10*, and *Il13* (Fig. 6b), suggesting that N-AC treatment might regulate the interconversion between progenitor and terminally differentiated T cells within the exhausted T cell pool. Indeed, flow cytometry analysis revealed that while N-AC treated, chronically stimulated T cells still expressed TOX, up to half of cells recovered expression of TCF-1, consistent with a transition from a terminally exhausted to a progenitor exhausted phenotype (Fig. 6c)[15, 38, 39]. More broadly, analysis of RNA-seq from N-AC treated chronically stimulated T cells demonstrated a global change in gene expression from genes associated with terminal exhaustion to progenitor-like T cells associated with self-renewal, including Quantitative PCR analysis confirmed that N-AC supplementation during chronic stimulation restored expression of key genes required for self-renewal in exhausted T cells, including *Tcf7* and *Myb*, while suppressing expression of genes associated with terminal T

cell exhaustion, such as *Prdm1* (Extended Data 7b)[40, 41, 42]. Notably, chronically stimulated T cells cultured in the presence of N-AC maintained elevated concentrations of intracellular calcium but decreased expression of NFAT target genes, suggesting that N-AC may prevent terminal T cell exhaustion by buffering Ca^{++}-driven, ROS-dependent NFAT activity (Extended Data 7c–d).

N-acetylcysteine reverses T cell effector dysfunction

While N-AC treatment restored T cell proliferation during chronic stimulation, the requirement of mitochondrial free radical production for full T cell activation and cytokine production raised the possibility that N-AC treated T cells might lack effector function[24]. However, we found that N-AC treatment actually increased cytokine production by chronically stimulated T cells, whereas immune checkpoint blockade was unable to do so (Fig. 7a). This rescue was dependent on ETC function, as N-AC was unable to rescue cytokine production during hypoxia (Extended Data 8a). Functionally, N-AC was able to improve the killing capacity of chronically stimulated T cells, and this capacity synergized with anti-PD-L1 therapy to fully restore T cell effector function (Fig. 7b). We also observed a synergistic effect of anti-PD-L1 therapy and N-AC on T cell metabolism, as anti-PD-L1 therapy, which is known to increase glucose uptake [43], increased mitochondrial oxygen consumption only in the presence of N-AC (Extended Data 8b–c). The ability of anti-oxidants to maintain T cell functionality was not restricted to N-acetylcysteine, as supplementation of T cells with either the mitochondrially-targeted antioxidant MitoTEMPO or the water-soluble Vitamin E analog Trolox similarly restored cytokine production in chronically stimulated T cells (Extended Data 8d).

We next sought to confirm whether induction of oxidative stress is limiting for T cells undergoing exhaustion *in vivo*. Intratumoral T cells *in vivo* exhibit a terminally differentiated phenotype marked by an inability to proliferate or produce effector cytokines as well as higher rates of apoptosis in response to *ex vivo* re-stimulation[8, 15, 44, 45]. We found that both tumor-infiltrating cells from mice bearing EL4 T cell lymphoma tumors[46] as well as CD19-directed CAR-T cells from mice bearing A20 B cell lymphoma tumors[47] exhibited impaired cytokine production and high rates of apoptosis upon *ex vivo* re-stimulation (Fig. 7c–f). N-AC treatment improved the viability and cytokine production of both endogenous and CAR-transduced exhausted T cells (Fig. 7c–f). These results demonstrate that oxidative stress limits the proliferative and functional capacity of T cells undergoing exhaustion *in vivo*. Finally, we evaluated whether buffering oxidative stress with N-AC could enhance anti-tumor T cell responses *in vivo*. In a B16 melanoma model, which is largely refractory to anti-PD-L1 therapy[48, 49], adoptive transfer of T cells cultured in the presence of N-AC improved the survival of tumor-bearing mice (Fig. 7g). Immunohistochemical analysis confirmed an improvement in the functional capacity of tumor-infiltrating T cells as reflected by an increase in Granzyme B expression (Fig. 7h). Collectively, these results demonstrate that N-AC reverses *in vivo* T cell effector dysfunction and enhanced anti-tumor immunity.

Discussion

While immune checkpoint inhibitors and CAR-modified T cell therapies have produced encouraging clinical responses in patients with cancer, persistent antigen exposure ultimately leads to terminal dysfunction of tumor-infiltrating T cells and limits immune-mediated tumor control. Recent findings demonstrating that successful response to anti-PD-1 therapy requires a subset of exhausted T cells that retain proliferative capacity[4, 6] strongly suggest that overcoming antigen-driven limitations on self-renewal are key to achieving durable anti-tumor immunity. Our laboratory previously established that during initial antigenic activation of T cells, both cytokine and CD28 stimulation promote nutrient uptake and catabolism to support cell growth and proliferation[9]. It remained unclear, however, what the metabolic effects of persistent antigenic stimulation would be and how such metabolic alterations might affect T cell proliferation and differentiation.

We now establish that altered metabolism resulting from persistent antigenic exposure is essential to limiting intratumoral T cell proliferation and self-renewal. The hallmark of this metabolic phenotype is a rapid induction of mitochondrial oxidative stress that limits the ability of T cells to engage in oxidative phosphorylation, resulting in bioenergetic limitations that are sufficient to block T cell proliferation. Moreover, we show that free radical-driven impairment of mitochondrial oxidative phosphorylation is both necessary and sufficient to repress gene expression programs associated with self-renewal while inducing gene expression programs associated with terminal T cell exhaustion.

The metabolic alterations observed in chronically stimulated T cells may underlie the phenotypic changes observed in immunotherapy failures. Failure to respond to immune checkpoint blockade is often associated with a depletion of T cells within the tumor parenchyma[50]. While this has been ascribed to mechanical barriers such as fibroblast-associated extracellular matrix, our findings suggest that intratumoral T cell depletion may actually reflect impaired survival under conditions known to promote redox dysfunction, including hypoxia and cysteine depletion. Another significant predictor of immunotherapy failure is a lack of TCF-1^{+} progenitor cells[4, 5, 8]. Our data demonstrate that chronic stimulation-dependent redox dysfunction suppresses TCF-1 expression and promotes a terminally exhausted phenotype that underlies checkpoint blockade unresponsiveness.

Recently, the transcription factor TOX was found to be essential for activation of the exhaustion-associated gene expression program, and T cells lacking *Tox* were more prone to terminal differentiation and death within tumors[20, 21, 22, 34]. Our data demonstrating that oxidative stress can promote *Tox* expression suggests that negative regulatory programs driven by TOX may protect T cells from bioenergetic catastrophe during chronic antigen exposure, permitting survival at the expense of effector capacity. Initial *Tox* expression and phenotypic exhaustion has been shown to require NFAT, but sustained *Tox* expression subsequently becomes calcineurin-independent[34]. Whether persistent calcium-driven mitochondrial ROS sustains *Tox* expression via NFAT-independent mechanisms remains to be determined.

Pharmacologic targeting of T cells to enhance immunotherapy has largely centered around blocking inhibitory immune checkpoints, which, while effective in many malignancies, is typically not durable. This may in part be because immune checkpoint blockade does not reprogram the chromatin landscape of exhausted T cells[15, 38, 39]. The underlying cause of epigenetic reprogramming during the development of intratumoral T cell dysfunction remains to be elucidated. However, our finding that reversing redox stress can reactivate gene expression even at loci known to be inaccessible in exhausted T cells suggests that even epigenetic silencing can be suppressed if mitochondrial redox damage is prevented. While these data provide evidence that drugs like N-acetylcysteine can restore and/or maintain an anti-tumor immune response *in vivo*, whether other therapies that preserve immune cell bioenergetic integrity can also help prevent T cell exhaustion remains to be explored.

METHODS

Cell Lines

B16-F10, B16-OVA, EL4, and A20 cell lines were all purchased from ATCC. B16-F10 and B16-OVA cell lines were cultured in DMEM + 10% FBS. EL4 and A20 cell lines were cultured in RPMI-1640 + 10% FBS + 2 mM L-glutamine + 50 μM β-mercaptoethanol (β-ME). All cells were tested routinely for mycoplasma and kept in culture for no more than 30 days or 15 passages.

Plasmids

LbNOX and MitoLbNOX were a gift from V. Mootha (Harvard) (Addgene plasmid #75285, 74448)[30] and were subcloned into pMIG-II vectors. All vectors were sequence confirmed using Sanger sequencing.

T cell isolation and activation

For activation of polyclonal $CD8^+$ T cells, T cells were isolated from the spleen and inguinal lymph nodes of C57BL/6 mice (Jackson 000664) using the Dynabeads Untouched $CD8^+$ T cell kit. T cells were activated with plate-bound anti-CD3 (2C11, 3 μg/mL, 3:1000 dilution) and anti-CD28 (19.51, 1 μg/mL, 1:500 dilution) for 48 h in RPMI-1640 media containing 10% FBS, 2 mM L-glutamine, 50 μM β-ME, and 10 ng/mL IL-2 (Peprotech). For activation of OT-I transgenic $CD8^+$ T cells, single cell suspensions were generated from spleens and inguinal lymph nodes of OT-I mice (Jackson 003831). Cells were cultured at 10×10^6 cells per mL in the presence of 1 μM SIINFEKL peptide (Invivogen) + for 48 h in RPMI-1640 media containing 10% FBS, 2 mM L-glutamine, 50 μM β-ME, and 10 ng/mL IL-2 (Peprotech).

Acute and chronic T cell stimulation

For OT-I transgenic T cells, following 48 h of initial stimulation as described above, T cells were co-cultured with B16-F10 melanoma cells that had been plated the day before at sub-confluent density in the presence of 1 ng/mL IFN-γ (Peprotech) to induce MHC-I expression. Cells were co-cultured at 1×10^6 T cells per mL in in RPMI-1640 media containing 10% FBS, 2 mM L-glutamine, 5 μM β-ME, and 10 ng/mL IL-2, with (chronic) or without (acute) the addition of 1 μM SIINFEKL. T cells were passaged into fresh co-

cultures every 48 h until eight days following initial stimulation, at which point cells were used for experiments. For polyclonal $CD8^+$ T cells, following 48 h of initial stimulation as described above, T cells were cultured at 1×10^6 cells per mL in in RPMI-1640 media containing 10% FBS, 2 mM L-glutamine, 5 μM β-ME, and 10 ng/mL IL-2 and with (chronic) or without (acute) plate-bound anti-CD3 (3 μg/mL, 3:1000 dilution). T cells were passaged onto fresh plates every 48 h until eight days following initial stimulation, at which point cells were used for experiments. $CoCl_2$ (Sigma) was resuspended in water and used at 10 μM. Rotenone (Cayman) was resuspended in DMSO and used at 100 nM. Oligomycin (Cayman) was resuspended in DMSO and used at 100 nM. N-Acetylcysteine (Sigma) was resuspended in water and used at 10 mM. Sodium Acetate (Sigma) was added directly to media to a concentration of 5 mM. MitoTEMPO (Cayman) was resuspended in DMSO and used at 100 nM. Trolox (Cayman) was resuspended in DMSO and used at 100 μM. Diamide (Sigma) was resuspended in water and used at 50 μM.

Retroviral infection

Mig-II plasmids were co-transfected with Moloney murine leukemia viral packaging plasmids (pCL-Eco, Addgene #12371, a gift from I. Verma Naviaux)[51] into 293T cells with polyethylenimine (PEI). Media was replaced 5 h later and supernatant containing viral particles was collected 36 h later. T cells were activated on plate-bound anti-CD3 and anti-CD28 as described above. 48 h later, spinfection was conducted with 1×10^6 cells in 1 mL containing polybrene at 8 μg/mL in an Eppendorf tube. Cells were used for experiments immediately thereafter.

In vitro killing assay

B16-OVA cells were plated at sub-confluent density (1×10^5 cells per plate). The following day, 1×10^5 T cells were added to wells containing adherent B16-OVA cells. 24 h later, T cells were washed off. 48 h later cells were counted using a Beckmann Coulter Counter.

Flow cytometry

Measurement of oxidative stress, lipid peroxidation, and mitochondrial mass —Cells were loaded with CM-H_2DCFDA (1 μM), MitoSOX Red (5 μM), BODIPY-C11 (5 μM), or MitoTracker Green (1 μM) for 30 minutes at 37°C in PBS. They were then quenched with RPMI containing 10% FBS, washed 2 times with FACS buffer, and analysed immediately using an LSR Fortessa machine (Beckman Dickinson) and FacsDiva software (v8.0). Analysis of mean fluorescence intensity was performed using FlowJo v10.0. All experiments were performed at least two independent times.

Measurement of viability, receptor expression and cytokine production—T cells were re-stimulated with phorbol myristate acetate (Sigma, 50 ng/mL) and ionomycin (Sigma, 500 ng/mL). 90 minutes later, cells were treated with Brefeldin A to block cytokine secretion. 3 h later, cells were stained for surface markers and simultaneously labelled with Live/Dead Blue Viability Dye (Thermo Fisher) for 20 minutes at 4°C. Cells were washed twice and fixed overnight using a FoxP3 Fixation/Permeabilization kit (Thermo Fisher). The following day, cells were washed and stained for intracellular cytokines at room temperature for 1 h. They were then washed 3 times and analysed using an LSR Fortessa machine

(Beckman Dickinson). Analysis of mean fluorescence intensity was performed using FlowJo v10.0. All experiments were performed at least two independent times. Antibodies used (at 1:100 unless otherwise noted) were TNF-PE (BioLegend, MP6-XT22, 506306), PD-1-PECy7 (BioLegend, RMP1–30, 109110) IFN-γ-FITC (BioLegend, XMG1.2, 505806), CD4-BV711 (BioLegend, RM4–5, 100550), CD8α-BV786 (BioLegend, 53–6.7, 100750), Tox-PE (Miltenyi, REA473, 130–120-716, 1:50), Tcf7-Alexa647 (Cell Signaling, C63D9, 6709), PD-L1-APC (BioLegend, 10F.9G2, 124312, 1:5000), LAG-3-PerCP-Cy5.5 (BioLegend, C9B7W, 125211), TIM-3-PE-Dazzle594 (BioLegend, B8.2C12, 134013).

Measurement of proliferation by Cell Trace Violet dilution—Naïve T cells were loaded with Cell Trace Violet (Invitrogen) as per manufacturer's instructions for 20 minutes at 37°C, quenched with media containing 10% FBS, and plated immediately for experiments. Proliferation was measured by fluorescence dilution using FlowJo v10.0.

Measurement of intracellular calcium levels by Indo-1 AM—T cells were loaded with Indo-1 AM (Invitrogen) as per manufacturer's instructions in serum-free media for 30 minutes at 37°C, quenched with media containing 10% FBS, and used immediately for flow cytometry experiments. Indo-1-bound and unbound fluorescence was assessed as per manufacturer's instructions on an LSR Fortessa. 1 μg of anti-CD3-biotin (145–2C11, 5 μg/mL, 1:100 dilution) and 2 μg of streptavidin were added as indicated. Ratios were calculated using FlowJo v10.0.

Growth curves

T cells were activated for 48 h as described above. They were subsequently plated in 24 well plates at 5×10^5 cells in 1 mL of RPMI-1640 media containing 10% FBS, 2 mM L-glutamine, 5 μM β-ME, and 10 ng/mL IL-2 and with (chronic) or without (acute) plate-bound anti-CD3 (3 μg/mL). Every two days for the duration of the experiment, cells were harvested, and cell number was counted using a Beckmann Coulter Counter with a cell volume gate of 75 – 4000 fL. 50% of the cells were then re-plated in 1 mL of media as described above. For nutrient deprivation experiments, cells were cultured in RPMI-1640 media without glucose, glutamine, or cysteine, 10% dialyzed FBS, 5 μM β-ME, 10 ng/mL of IL-2, and the indicated concentrations of glucose, glutamine, and cysteine, with (chronic) or without (acute) plate-bound anti-CD3 (3 μg/mL, 3:1000 dilution). All experiments were performed at least two independent times.

Quantification of gene expression

RNA was isolated from T cells using Trizol (Invitrogen) according to manufacturer instructions and 200 ng RNA was used for cDNA synthesis using iScript (BioRad). Quantitative real-time PCR analysis was performed in technical triplicate using QuantStudio 7 Flex (Applied Biosystems) with Power SYBR Green (Life Technologies). All data were generated using cDNA from triplicate wells for each condition. Actin was used as an endogenous control for all experiments. Primers used for qRT-PCR are shown in Supplementary Table 1. For RNA-sequencing, RNA was isolated from T cells using Trizol and then prepared as instructed using the TruSeq RNA Sample Preparation Kit v2 (Illumina) in accordance with the manufacturer's instructions. RNA-seq samples were sequenced using

Illumina NextSeq 500 generating 150-bp paired-end reads. Fastq files were aligned to genome build mm9 using TopHat2 v2.1.1 with default parameters. Aligned features were counted with htseq-count v0.11.1 and differential expression was determined using the edgeR package v3.28.1 in Bioconductor v3.10 as previously described[52].

Gene set enrichment analysis

Gene set enrichment analysis (GSEA)[53] was performed using pre-ranked gene lists. GSEA Preranked version 6.0.12 was used with default parameters and data were exported and graphed in GraphPad Prism version 8.

Single cell RNA-Seq analysis

Gene expression UMI counts for single cells were used as generated previously[6, 19] and further normalized by dividing by the total counts for that cell, multiplied by a scale factor of 10,000 and log1p normalized using the NormalizeData function in Seurat v2.3.4[54]. The glycolysis score for each cell was calculated as the average *z*-score over all genes in the HALLMARK_GLYCOLYSIS gene set[55]. ROS score for each cell was calculated as the average *z*-score of all genes in the GO_RESPONSE_TO_OXIDATIVE_STRESS gene set[56]. NFAT score for each cell was calculated as the average *z*-score over all genes in the PID_NFAT_TFPATHWAY gene set[57]. TCR annotation was performed as described previously[5]. Single cells were grouped by TCR clonotype based on matching TRB amino acid sequence. P values were calculated using a one-sided Student's t-test.

Nutrient consumption and secretion

Cells were plated in 12-well plates at 5×10^5 cells/well and treated and/or stimulated as indicated in the figures while keeping cell density at sub-confluency. Media was exchanged for the assay period of 24 h, then collected, centrifuged at 300*g* for 3 min to remove cellular components and analyzed using a 2950D Biochemistry Analyzer (YSI Life Sciences) to determine glucose, glutamine and lactate concentration. Absolute rates of consumption/secretion of these metabolites were calculated by subtracting their concentrations in media incubated for the same amount of time without the cells, then normalized to the cell number, media volume and hours of incubation. These experiments were performed independently at least two times.

NADH/NAD$^+$ levels

NADH and NAD+ levels were measured using a modified version of manufacturer instructions supplied with the NAD/NADH-Glo Assay (Promega) as previously described [23]. Briefly, T cells were acutely and chronically stimulated as described above prior to preparation of cell extracts. For extraction, cells were washed 3 times in ice-cold PBS, extracted in 100 μL ice-cold lysis buffer (1% Dodecyltrimethylammonium bromide (DTAB) in 0.2 N NaOH diluted 1:1 with PBS), and immediately frozen at −80°C. To measure NADH, 20 μL of sample was incubated at 75°C for 30 min to selectively degrade NAD$^+$. To measure NAD$^+$, 20 μL of the sample was combined with 20 μL lysis buffer and 20 μL 0.4 N HCl and incubated at 60°C for 15 min to degrade NADH. Following incubations, samples were allowed to equilibrate to room temperature and then quenched by neutralizing with 20

μL 0.25 M Tris in 0.2 N HCl (NADH) or 20 μL 0.5 M Tris base (NAD^+). Manufacturer instructions were followed thereafter to measure NADH/NAD^+ using a luminometer.

Extracellular flux analysis

Extracellular acidification rate (ECAR) and oxygen consumption rate (OCR) were measured using a Seahorse XFe96 Extracellular Flux Analyzer (Agilent Technologies). Cells were plated on Cell-Tak (Fisher) coated XF 96-well plates at 2×10^5 cells per well in assay media (DMEM supplemented with 10 mM glucose, 2 mM L-glutamine, and 1 mM sodium pyruvate) as previously described[58]. Analysis of the extracellular acidification rate and oxygen consumption rate were performed at basal level, and after subsequent injections of oligomycin (1 μM), carbonyl cyanide p-trifluoromethoxyphenylhydrazone (FCCP; 1 μM), and rotenone/antimycin mix (0.5 μM). Where included, acute injection of anti-CD3/anti-CD28 coated beads preceded the injection of oligomycin. In some experiments, 2-deoxy-D-glucose (2-DG) was injected at a final concentration of 5 mM. Following measurements, cell number was determined, averaged per condition, and the extracellular acidification and oxygen consumption rates normalized to these values. Mitochondrial ATP production was calculated by subtracting the minimum respiration rate following oligomycin injection from the final respiration rate prior to oligomycin injection.

Immunoblotting

Protein lysates were extracted in RIPA buffer (Cell Signaling), separated by SDS-PAGE and transferred to nitrocellulose membranes (Bio-Rad). Membranes were blocked in 5% milk in Tris (pH)-buffered saline with 0.1% Tween-20 (TBST) and incubated at 4°C with primary antibodies overnight. After TBST washes the next day, membranes were incubated with horseradish-peroxidase conjugated secondary antibodies (GE Healthcare, GENA931 or GENA934, 1:5000) for 1 h, incubated with ECL (Pierce or GE Healthcare) and imaged using a ChemiDoc Touch Imaging System (Bio-Rad). Antibodies used (at 1:1,000 unless otherwise noted) were FLAG (Sigma-Aldrich, F1804), total OXPHOS (Abcam, ab110413), Glut1 (Cell Signaling, 12939S), and Actin (Sigma, A3854 at 1:20,000).

Metabolomic analyses

Stable isotopologue labeling and metabolite extraction—T-cells were acutely or chronically stimulated for 8 days as described above. On day 8 following stimulation, cells were washed with PBS and re-plated on plates coated with anti-CD3 (3 μg/mL, 3:1000 dilution) in fresh RPMI-1640 containing 10% FBS (for metabolic profiling studies) or 10% dialyzed FBS (for isotopologue tracing studies), 1% penicillin-streptomycin, 2 mM L-glutamine, 5 μM BME, and 10 ng/mL IL-2. For isotopologue tracing studies RPMI-1640 without glucose or glutamine was used, supplemented with either ^{12}C-glucose (Sigma) and ^{12}C-glutamine (Gibco) or the ^{13}C versions of each metabolite, [U-^{13}C] glucose or [U-^{13}C] glutamine (Cambridge Isotope Laboratories) to a final concentration of 10 mM (glucose) and 2 mM (glutamine). For [U-^{13}C] palmitate (Sigma) isotopologue tracing studies, ^{12}C or [U-^{13}C] palmitate was resuspended in 100% ethanol at 250 mM and conjugated to 10% BSA at a 3:1 ratio and added to RPMI-1640 media at a final concentration of 100 μM. 6 h later, cells were collected, centrifuged at 300*g* for 2 min at 4°C, and resuspended in 1 mL of

ice-cold 80% methanol containing 2 μM deuterated 2-hydroxyglutarate (D-2-hydroxyglutaric-2,3,3,4,4-d_5 acid, d5–2HG) as an internal standard (for GC-MS analyses) or 1.5 μM $^{13}C^{15}N$ labeled amino acids (Cambridge isotope laboratories) as internal standards (for LC-MS metabolomic profiling). For isotoplogue tracing studies by LC-MS, 80% methanol was used for metabolite extraction. After overnight incubation at −80°C, samples were vortexed and centrifuged at 20,000*g* for 20 min to remove protein. Supernatants were dried in a vacuum evaporator (Genevac EZ-2 Elite) for 3 h.

Metabolite profiling, TCA intermediates steady state levels and isotopologue analysis—For GC-MS analysis of tricarboxyclic acid cycle (TCA) cycle intermediates (profiling and stable isotope tracing) samples were incubated in 50 μL of 40 mg/mL methoxyamine hydrochloride (Sigma) in pyridine (Sigma) at 30°C for 2 h, and derivatized with addition of 80 μL of MSTFA + 1% TCMS (Thermo Scientific) and 70 μl ethyl acetate (Sigma) with shaking at 37°C for 30 minutes. Samples were analyzed using an Agilent 7890A GC coupled to Agilent 5977C mass selective detector with operating parameters set as described before[59]. Peaks representing compounds of interest were extracted and integrated using MassHunter software (Agilent Technologies) and normalized to the internal standard (d5–2HG) peak area. Ions used for quantification of metabolite levels were as follows: d5–2HG *m/z* 354; αKG, *m/z* 304; aspartate, *m/z* 334; citrate, *m/z* 465; fumarate, *m/z* 245; glutamate, *m/z* 363; malate, *m/z* 335 and succinate, *m/z* 247. All peaks were manually inspected and verified relative to known spectra for each metabolite. Enrichment of ^{13}C was assessed by quantifying the abundance of the following ions: aspartate, *m/z* 334–346; citrate, *m/z* 465–482; fumarate, *m/z* 245–254; glutamate, *m/z* 363–377 and malate, *m/z* 335–347. Correction for natural isotope abundance was performed using IsoCor software[60].

For metabolomic profiling and isotopologue tracing studies using LC-MS, dried extracts were resuspended in either 60 μL of 60% acetonitrile in water or in 40 μL of 97:3 water:methanol containing 10 mM tributylamine and 15 mM acetic acid for HILIC or ion pair LC separations respectively. Samples were vortexed, incubated on ice for 20 min, and clarified by centrifugation at 20,000*g* for 20 min at 4°C. HILIC LC-MS analysis was performed on 6545 Q-TOF mass spectrometer (Agilent Technologies) in both positive and negative ionization mode using columns, buffers and LC-MS parameters as described previously[61]. Targeted data analysis, isotopologue extraction and natural isotope abundance correction was performed using MassHunter Profinder software v10.0 (Agilent Technologies). For profiling experiments, peak areas of $^{13}C^{15}N$ labeled amino acids internal standards were analyzed to confirm <10% of inter-sample variability. Ion pair LC-MS analysis was performed with LC separation on a Zorbax RRHD Extend-C18 column (150 mm × 2.1 mm, 1.8 μm particle size, Agilent Technologies), and using gradient of solvent A (10 mM tributylamine and 15 mM acetic acid in 97:3 water:methanol) and solvent B (10 mM tributylamine and 15 mM acetic acid in methanol) according to the manufacturer's instructions (MassHunter Metabolomics dMRM Database and Method, Agilent Technologies).

Labeling of lipids by ^{14}C-glucose

T cells were acutely or chronically stimulated as described above. 4 days after initial stimulation, cells were plated in 24 well plates at 5×10^5 cells in 1 mL of RPMI-1640 media without glucose containing 10% dialyzed FBS, 2 mM L-glutamine, 5 μM BME, 10 ng/mL IL-2, 10 mM glucose and 0.5 μCi/mL [U-^{14}C]glucose (Perkin Elmer) and with (chronic) or without (acute) plate-bound anti-CD3 (3 μg/mL). 24 h later, cells were washed twice with PBS and lipids were harvested with 50% methanol containing 0.1M HCl on dry ice, extracted with chloroform, and transferred to scintillation vials. A Perkin Elmer Tri-Carb 2910 TR scintillation counter was used to measure ^{14}C counts per minute (CPM) for one minute per sample. CPM were normalized to cell number measured from duplicate samples.

Animal models

All animal experiments were performed according to Memorial Sloan Kettering Cancer Center Institutional Animal Care and Use Committee (IACUC) guidelines (Protocol Number 11–03-007, Animal Welfare Assurance Number FW00004998).

In vivo tumor models—C57BL/6 scid (Jackson 001913) mice were injected subcutaneously with 2×10^5 B16-OVA cells in a 1:1 mix of PBS and Matrigel (Corning). 5 days later, 2×10^6 OT-I T cells that had been acutely or chronically stimulated in the presence or absence of N-AC as described above were adoptively transferred to mice via retro-orbital injection. All mice were treated with blocking antibodies against anti-PD-L1 (10F.9G2, BioXCell, 200 ug twice weekly). Mice were monitored daily and were sacrificed for signs of morbidity. At the time of sacrifice, tumors were fixed in 4% paraformaldehyde and sequentially dehydrated in ethanol. Paraffin embedding and immunohistochemistry for Granzyme B was performed by HistoWiz. Kaplan-Meier analysis of survival was performed using GraphPad PRISM 8 software.

Ex vivo analysis of tumor-infiltrating T cells—C57BL/6 mice were injected subcutaneously with 2×10^5 EL4 cells in a 1:1 mix of PBS and Matrigel (Corning). 14 days later, tumors were harvested and single cell suspensions were generated by manual dissociation. Cells were then re-stimulated on 6-well plates coated with anti-CD3 (3 μg/mL, 3:1000 dilution) in 2 mL of RPMI-1640 media containing 10% FBS, 2 mM L-glutamine, 5 μM β-ME, and 10 ng/mL IL-2 and with or without N-AC (10 mM). 3 days later, cells were re-stimulated with PMA and ionomycin and assessed for expression of CD8, PD-1, TNF, and IFN-γ as described above.

CAR-T cell models—CD19-specific CAR-T cells were generated as previously described [47]. The CAR constructs included an scFv, composed of a mouse CD8 signal peptide, IgH rearrangement, glycine–serine linker, and IgL rearrangement. The scFv was fused to the mouse CD8 hinge, the transmembrane region, and mouse stimulatory domains, including mouse CD28 and/or mouse CD3ζ. The m1928z construct was cloned into pENTR1A in frame followed by a sequence encoding the E2A self-cleaving peptide. For CAR-T cell generation, activated splenic T cells were spinfected with virus containing the m1928z-encoding construct. For CAR-T cell experiments, we utilized an HSCT-based allogeneic strategy with an MHC-disparate model (B6→BALB/c) as previously described[47]. Irradiated

BALB/c recipients received B6 bone marrow, 1×10^6 A20 lymphoma cells, and 1×10^6 CAR-T cells intravenously via tail vein injection. 14 days later, spleens were harvested, and CAR-T cells were isolated based on GFP expression using a Sony SH800 sorter. Following sorting, cells were re-stimulated on 6-well plates coated with anti-CD3 (3 μg/mL, 3:1000 dilution) in 2 mL of RPMI-1640 media containing 10% FBS, 2 mM L-glutamine, 5 μM β-ME, and 10 ng/mL IL-2 and with or without N-AC (10 mM). 3 days later, cells were re-stimulated with PMA and ionomycin and assessed for expression of CD8, PD-1, TNF, and IFN-γ as described above.

Statistical analysis

GraphPad PRISM 8 software was used for statistical analyses. Error bars, p-values and statistical tests are reported in figure legends.

Data availability

Datasets are deposited in the NCBI Gene Expression Omnibus using the following accession numbers: RNA-seq, GSE138459. Additional information can be found in the Life Sciences Reporting Summary. Further information and requests for reagents may be directed to, and will be fulfilled by, the corresponding authors, Craig B. Thompson (thompsonc@mskcc.org).

Extended Data

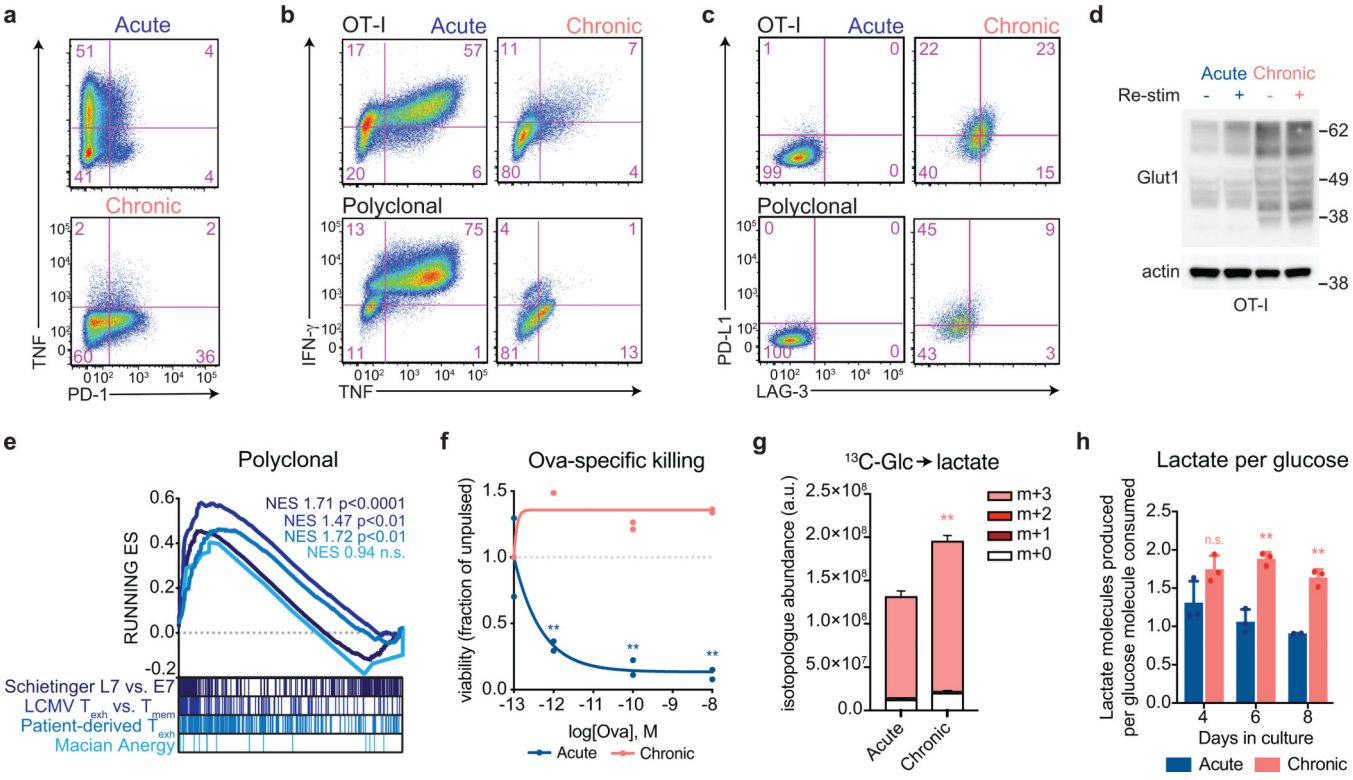

Extended Data Fig. 1. Chronic T cell stimulation induces T cell exhaustion.

All experimental analyses were conducted eight days after initial stimulation unless otherwise specified. (a-c) Expression of inhibitory immunoreceptors (PD-1, LAG-3, PD-L1) and intracellular cytokine production (IFN-γ and TNF) in acutely and chronically stimulated T cells following re-stimulation with PMA and ionomycin. (d) Expression of Glut1 in acutely or chronically stimulated OT-I T cells with or without restimulation using bead-bound anti-CD3. Actin is used as a loading control. Experiment was repeated three times with similar results. Uncropped blot can be found within Source Data. (e) Gene set enrichment plot showing that genes associated with chronically stimulated polyclonal T cells *in vitro* are enriched for genes upregulated in exhausted CD8+ T cells (Texh) but not anergic T cells[15]. (f) Killing of peptide-pulsed B16 cells. Luciferase-expressing B16 cells pulsed with Ova peptide at the indicated doses for 4 h were co-cultured with acutely or chronically stimulated T cells for 24 h. The following day, cells were lysed and luciferase expression was assessed using a luminometer. (g) Normalized isotopologue abundance of intracellular lactate in acutely and chronically stimulated T cells following 6 h of re-stimulation by plate-bound anti-CD3 in the presence of U-^{13}C-Glucose. Abundance was normalized to cell number at the time of harvest. (h) Median lactate excreted per molecule of glucose consumed in acutely and chronically stimulated T cells following initial stimulation. *P* values were calculated by unpaired, two-sided Student's *t*-test (f-h) relative to acutely stimulated T cells or based on 1,000 permutations by the GSEA algorithm and not adjusted for multiple comparisons (e). Data are presented as the mean ± s.d. of n=3 biologically independent samples from a representative experiment. **P<0.01.

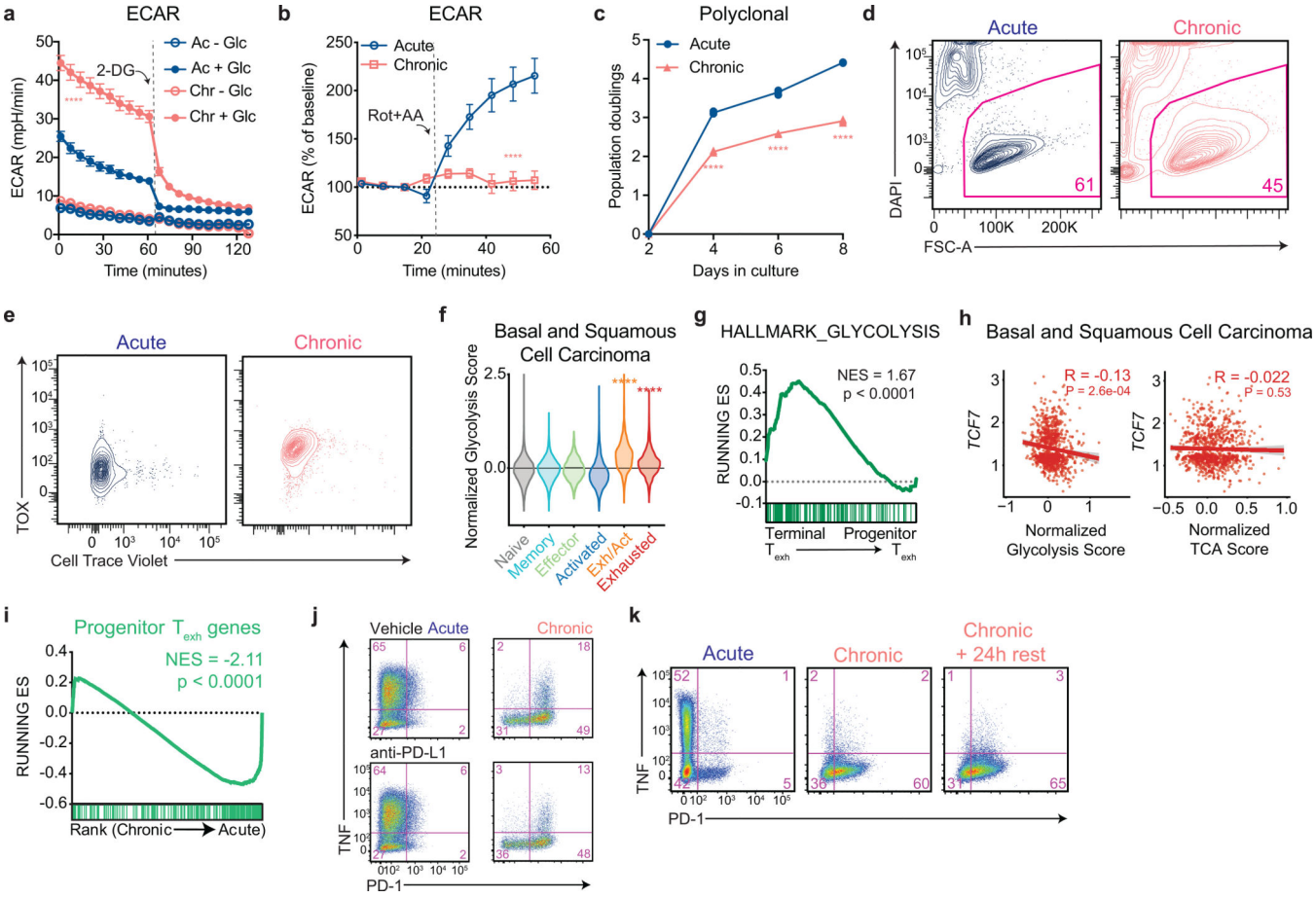

Extended Data Fig. 2. Aerobic glycolysis is a hallmark of chronic stimulation-dependent terminal T cell dysfunction.

(a) Extracellular acidification rate of acutely and chronically stimulated polyclonal T cells in media containing or lacking glucose as indicated. (b) Extracellular acidification rate of acutely and chronically stimulated polyclonal T cells at baseline and in response to electron transport chain inhibition. (c) Population doublings of acutely and chronically stimulated polyclonal CD8+ T cells following initial stimulation. (d) Viability of acutely and chronically stimulated T cells as determined by forward scatter and DAPI exclusion. (e) Intracellular TOX expression and proliferation as measured by dilution of Cell Trace Violet fluorescence of acutely or chronically stimulated T cells. (f) Normalized expression of glycolytic genes in CD8+ T cell clusters from patients with basal and squamous cell carcinoma treated with immune checkpoint blockade[19]. (g) Gene set enrichment plot showing that genes associated with terminally exhausted T cells isolated from murine B16 melanoma tumors[8] are enriched for glycolytic genes. (h) Correlation of glycolysis score (left) and TCA cycle score (right) with *TCF7* expression in exhausted CD8$^+$ T cell clusters from basal and squamous cell carcinoma patients treated with immune checkpoint inhibitors[6]. (i) Gene set enrichment plot showing that chronically stimulated OT-I T cells *in vitro* significantly downregulate genes upregulated in progenitor T_{exh} as compared to terminal T_{exh}[8]. (j-k) Intracellular cytokine production in acutely and chronically stimulated polyclonal T cells following re-stimulation. In (j), cells were cultured in the presence or

absence of anti-PD-L1 (10F.9G2) from D2-D8. In (k), “Chronic + 24h rest” cells were rested in the absence of plate-bound anti-CD3 for 24 h prior to re-stimulation. Experiment was repeated three times with similar results. *P* values were calculated by unpaired, two-sided Student’s *t*-test (a-c) relative to acutely stimulated T cells or based on 1,000 permutations by the GSEA algorithm and not adjusted for multiple comparisons (f-i). Data are presented as the mean ± s.d. of n=3 biologically independent samples from a representative experiment. ****P<0.0001.

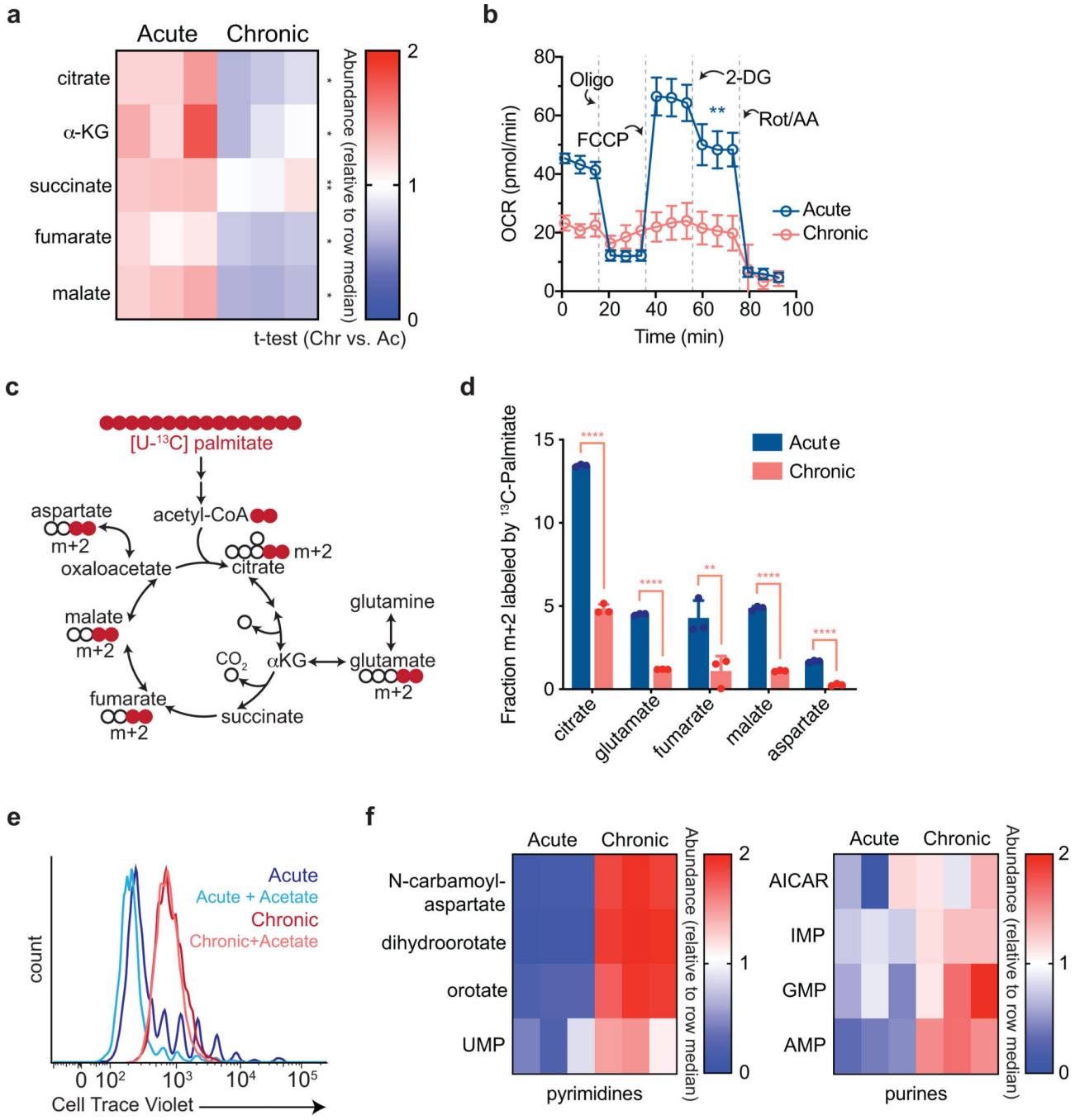

Extended Data Fig. 3. Chronic antigen stimulation impairs mitochondrial oxidation and ATP production.

(a) Quantification of relative tricarboxylic acid cycle metabolite pool sizes in acutely and chronically stimulated T cells. Columns represent biological replicates for each condition. (b) Oxygen consumption rate (OCR) of acutely or chronically stimulated T cells at baseline or in the presence of ATP synthase inhibition (Oligo), uncoupling agents (FCCP), inhibition of glucose uptake (2-DG), and complex III/IV inhibition (Rot/AA). (c) Schematic depicting how oxidative metabolism of uniformly-labeled palmitate ([U-^{13}C] palmitate) generates metabolites associated with the TCA cycle. Colored circles represent ^{13}C-labeled carbons.

(d) Fractional labeling by [U-^{13}C] palmitate of citrate, glutamate, fumarate, malate and aspartate in acutely and chronically stimulated T cells following re-stimulation. (e) Proliferation of T cells acutely or chronically stimulated in the presence or absence of supplemental sodium acetate (5 mM), as measured by dilution of Cell Trace Violet fluorescence. (f) Quantification of pool sizes of metabolite intermediates in nucleotide synthesis in acutely and chronically stimulated T cells. Heatmap depicts pool size relative to row median. Columns represent biological replicates for each condition. Experiment was repeated two times with similar results. *P* values were calculated by unpaired, two-sided Student's *t*-test (a,b,d). Data are presented as the mean ± s.d. of n=3 biologically independent samples from a representative experiment. **P<0.01. ****P<0.0001.

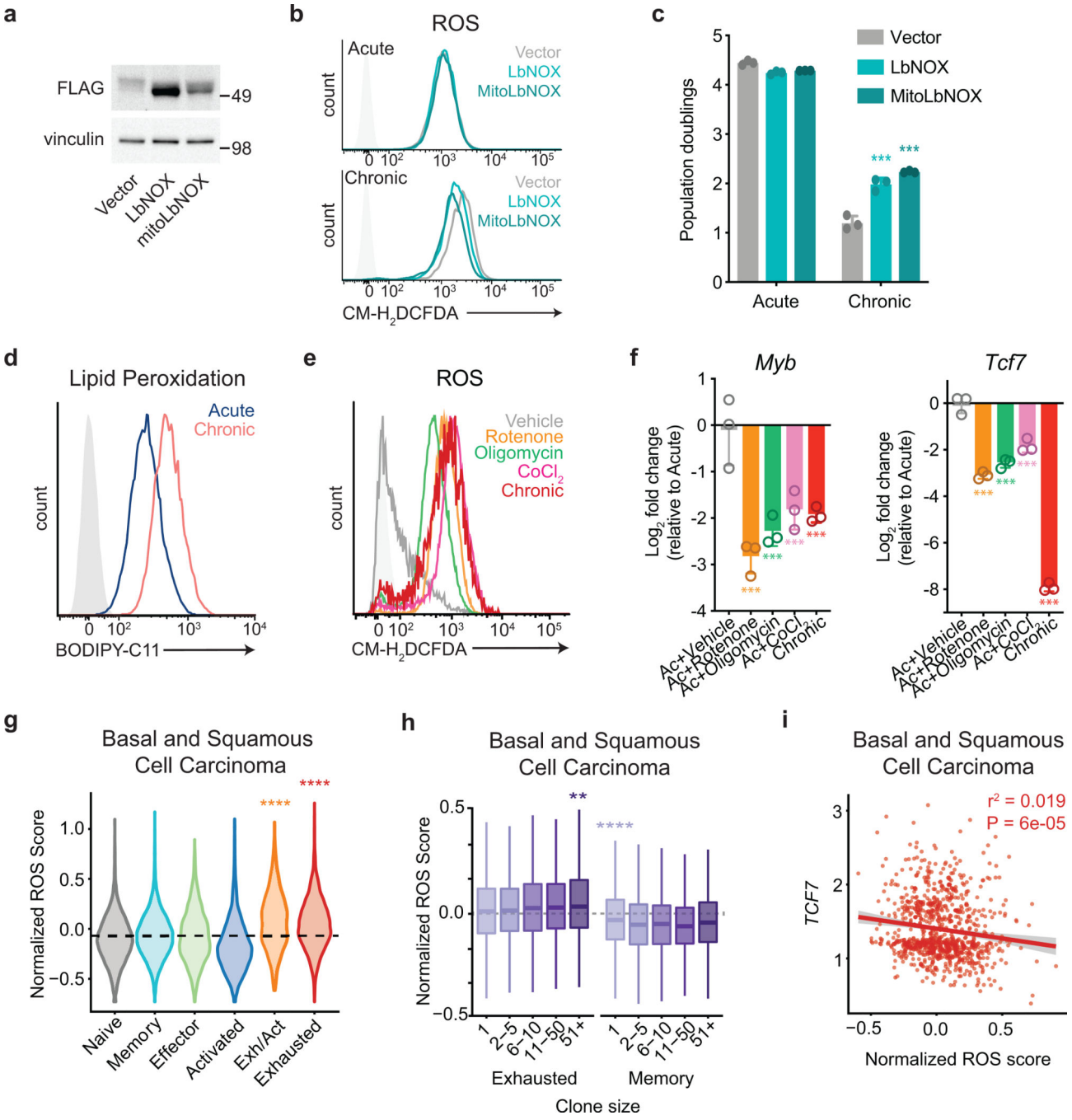

Extended Data Fig. 4. Oxidative stress limits T cell proliferative capacity.

(a) Western blot depicting overexpression of FLAG-tagged recombinant NADH oxidase enzymes LbNOX and MitoLbNOX in T cells[30]. Experiment was repeated three times with similar results. Uncropped blot can be found within Source Data. (b) Fluorescence intensity of acutely and chronically stimulated T cells expressing vector control, LbNOX, or MitoLbNOX following eight days in culture after loading with CM-H_2DCFDA. (c) Population doublings of acutely and chronically stimulated T cells expressing vector control, LbNOX, or MitoLbNOX. (d) Fluorescence intensity of acutely and chronically stimulated T

cells after loading with BODIPY-C11 to measure lipid peroxidation. Light-grey-shaded peak represents negative control. (e) Fluorescence intensity of acutely or chronically stimulated T cells cultured with or without pharmacologic agents that impair ETC function following 2 days of initial stimulation. Cells were loaded with CM-H_2DCFDA to measure ROS on D8 following initial stimulation. (f) qRT-PCR of *Myb* and *Tcf7* in acutely or chronically stimulated T cells with or without the addition of the indicated agents for 6 days following 2 days of primary stimulation. (g-i) Expression of oxidative stress-related metabolic genes ("ROS score") in tumor-infiltrating CD8+ T cells from basal and squamous cell carcinoma patients treated with immune checkpoint inhibitors[19]. In (g), ROS score in independent CD8+ T cell clusters is shown. In (h), ROS score in exhausted and memory T cell populations is shown according to clone size as measured by TCR sequencing; box center line=median, box limits=upper and lower quartiles, box whiskers=1.58 x interquartile range. In (i), correlation of ROS score with *TCF7* expression in exhausted CD8+ T cells is shown. Only cells with non-zero *TCF7* expression were included. *P* values were calculated by one-way ANOVA with Sidak's multiple comparisons post-test (g,i), or one-sided Student's *t*-test relative to base mean (g-h). Data are presented as the mean ± s.d. of n=3 biologically independent samples from a representative experiment. **P<0.01. ***P<0.001. ****P<0.0001.

a

Rank	Motif	P-value	% of targets	% of bg	Best Match/Details
1		1e-869	35.7%	8.6%	BATF(bZIP)/Th17-BATF-ChIP-Seq(GSE39756)/Homer(0.985)
2		1e-780	37.6%	10.6%	NFAT(RHD)/Jurkat-NFATC1-ChIP-(Jolma et al)/Homer(0.969)
3		1e-312	40.3%	20.55%	Ets1-distal(ETS)/CD4+-PolII-ChIP-Seq(Barski et al)/Homer(0.962)
4		1e-265	15.8%	4.74%	Nur77(NR)/K562-NR4A1-ChIP-Seq(GSE31363)/Homer(0.966)
5		1e-247	38.8%	21.23%	RUNX(Runt)/HPC7-Runx1-ChIP-Seq(GSE22178)Homer(0.983)

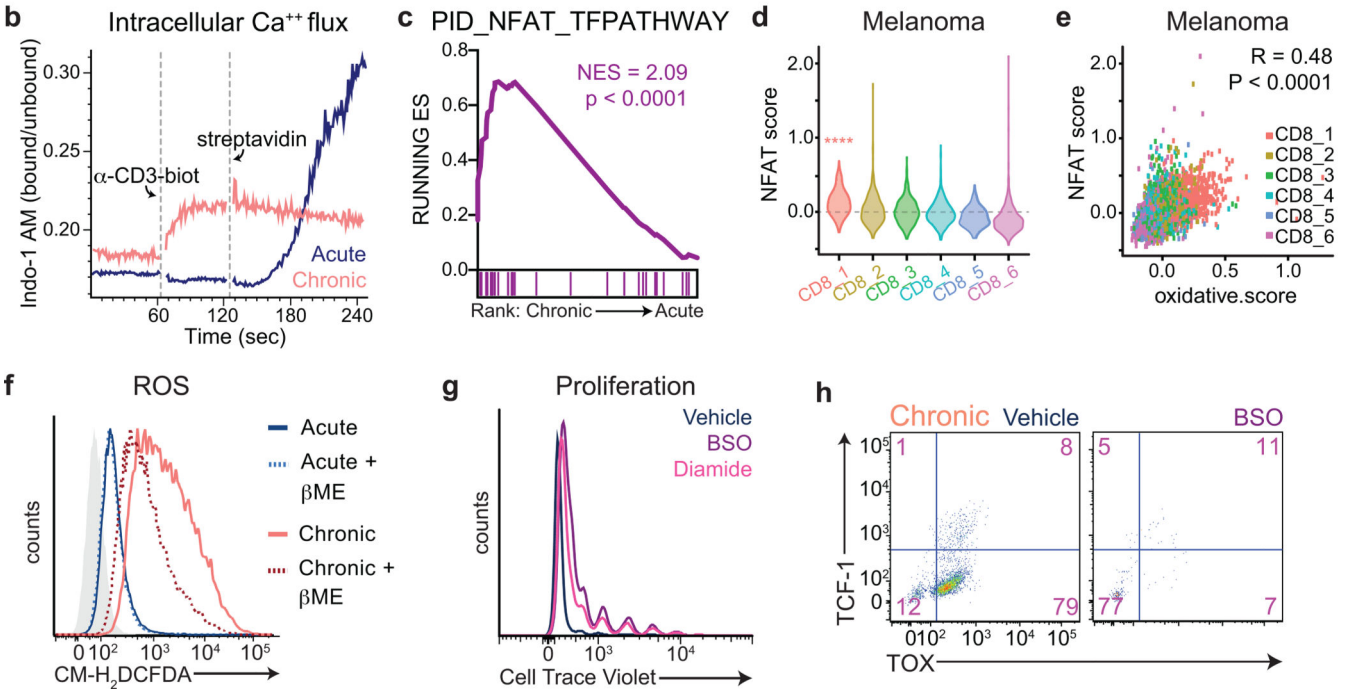

Extended Data Fig. 5. Endogenous antioxidant production is limiting for T cell proliferation.

(a) Motif analysis of sites with increased accessibility in tumor-infiltrating CD8+ T cells (L7) as compared to T cells from Listeria-infected mice (E7) showing NFATc1 as among the motifs whose accessibility was most preferentially increased in L7 cells[15]. (b) Intracellular calcium flux as measured by ratio of bound to unbound Indo-1-AM in acutely and chronically stimulated T cells, at baseline, in response to monomeric anti-CD3, and in response to receptor clustering (streptavidin). (c) Gene set enrichment plot showing that chronically stimulated OT-I T cells are enriched for NFAT target genes. (d) Expression of NFAT target genes ("nfat score") in independent CD8+ T cell clusters. (e) Correlation of expression of NFAT target genes ("nfat score") with expression of oxidative stress-related metabolic genes ("ROS score") in tumor-infiltrating CD8+ T cells from melanoma patients treated with immune checkpoint inhibitors. (f) Fluorescence intensity of acutely and chronically stimulated T cells cultured with or without βME supplementation after loading with CM-H_2DCFDA to measure ROS. Light-grey-shaded peak represents negative control. (g) Proliferation of T cells acutely stimulated in the presence or absence of BSO or diamide as measured by dilution of Cell Trace Violet fluorescence. (h) Expression of TCF-1 and

TOX in chronically stimulated T cells cultured in the presence or absence of BSO. *P* values were calculated by one-sided Student's *t*-test relative to base mean (d-e). ****P<0.0001

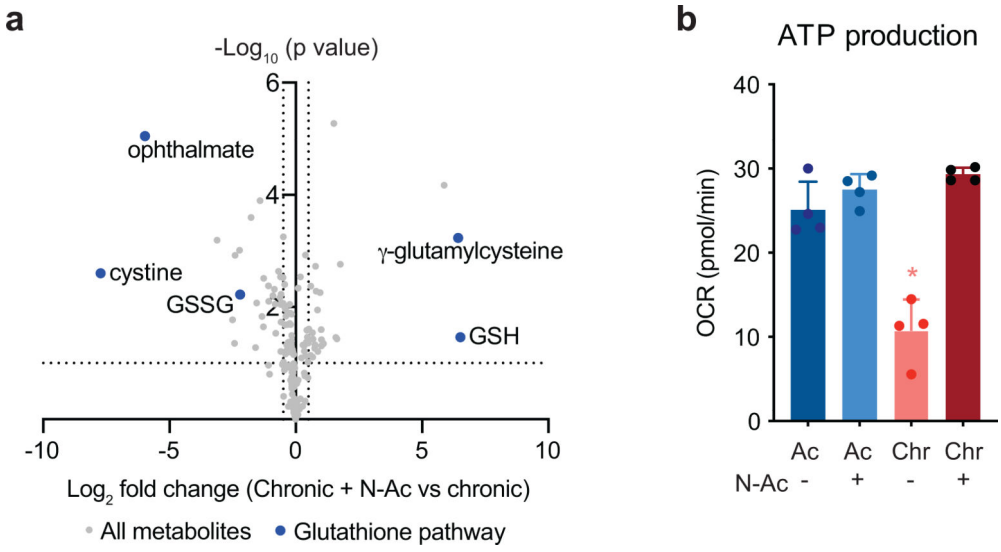

Extended Data Fig. 6. N-acetylcysteine reverses oxidative stress in chronically stimulated T cells.

(a) Quantification of relative metabolite pool sizes as measured by LC-MS in chronically stimulated T cells cultured with or without N-AC. Colored dots represent intermediates in glutathione synthesis as indicated. Dashed lines represent cutoffs of $p < 0.01$ and $\log_2$ fold change > 0.5. (b) ATP production by acutely or chronically stimulated T cells cultured with or without N-AC. *P* values were calculated by one-way ANOVA with Sidak's multiple comparisons post-test compared to acutely stimulated T cells (b). Data are presented as the mean ± s.d. of n=4 biologically independent samples from a representative experiment (b). *P<0.05.

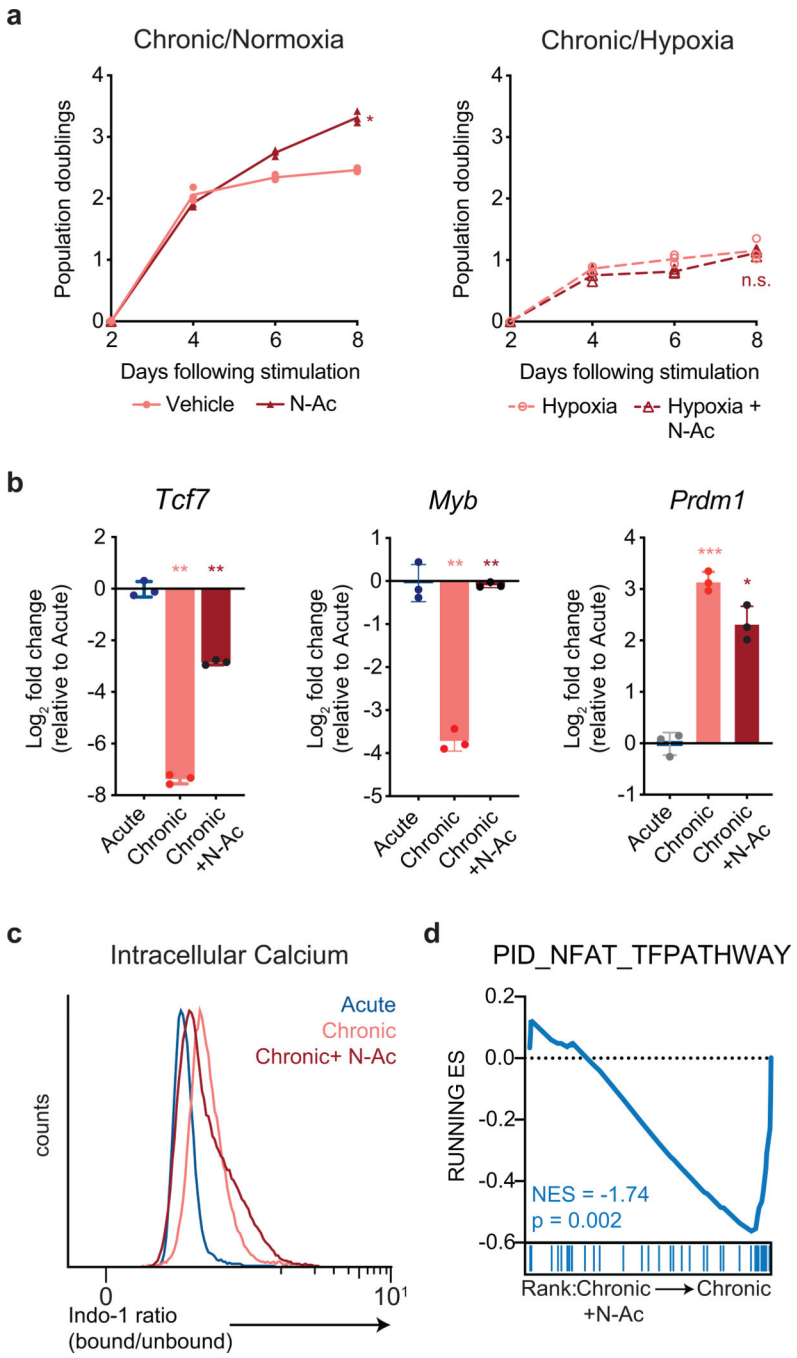

Extended Data Fig. 7. Antioxidants restore T cell self-renewal during chronic stimulation.

(a) Population doublings of chronically stimulated T cells with or without N-AC supplementation under normoxic (left) or hypoxic (right) conditions. Experiment was repeated two times with similar results. (b) qRT-PCR of *Tcf, Myb,* and *Prdm1* in acutely or chronically stimulated T cells with or without the addition of N-AC as indicated. (c) Intracellular calcium flux as measured by ratio of bound to unbound Indo-1-AM in acutely and chronically stimulated T cells cultured with or without N-AC. (d) Gene set enrichment plot showing that the addition of N-AC during chronic stimulation reduces expression of

NFAT target genes. *P* values were calculated by unpaired, two-sided Student's *t*-test relative to cells cultured without N-AC (a), one-way ANOVA with Sidak's multiple comparisons post-test (b) or based on 1,000 permutations by the GSEA algorithm and not adjusted for multiple comparisons (d). Data are presented as the mean ± s.d. of n=3 biologically independent samples from a representative experiment. *P<0.05. **P<0.01. ***P<0.0001.

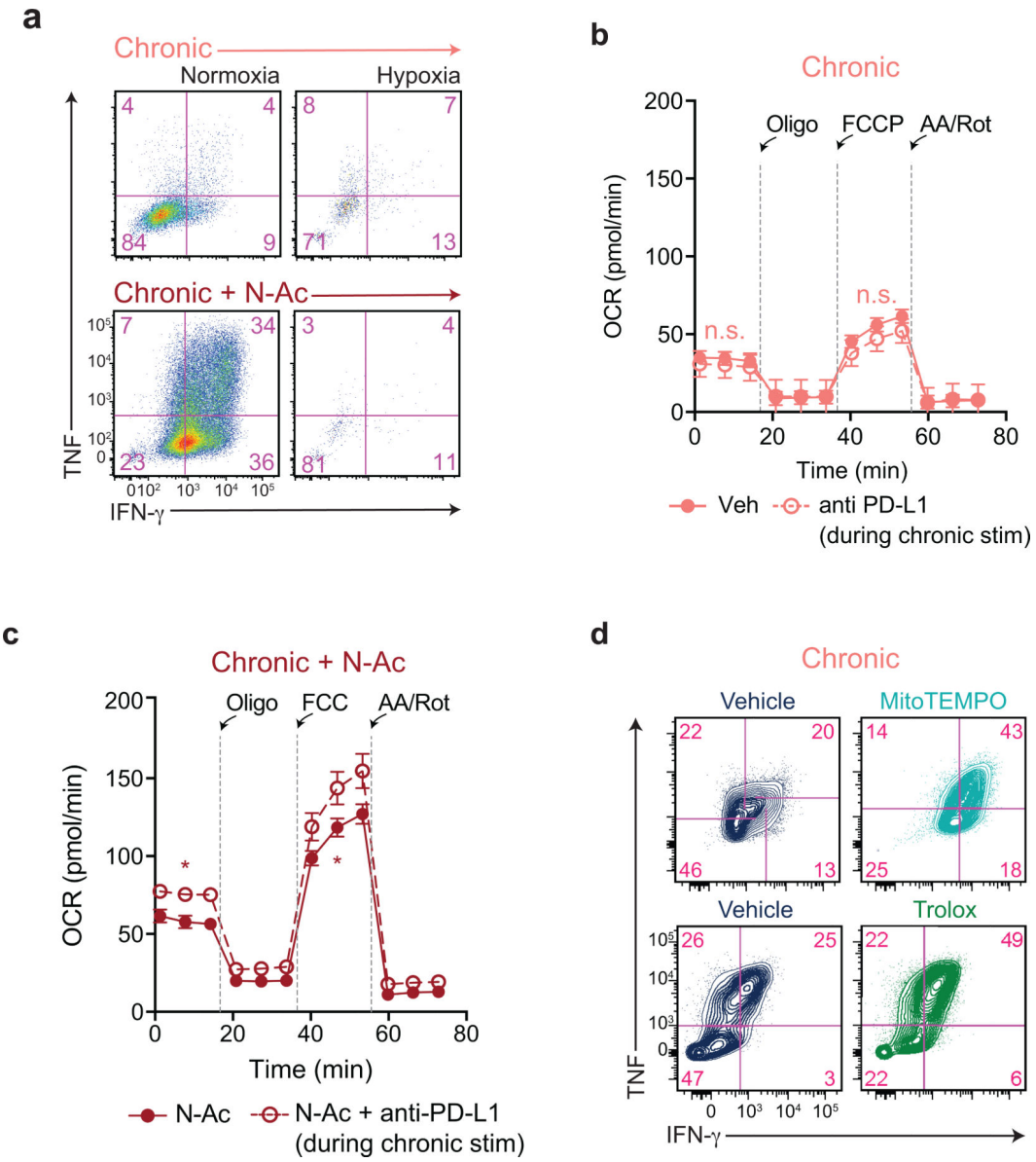

Extended Data Fig. 8. Antioxidants reverse endogenous tumor-associated T cell dysfunction.

(a) Production of IFN-γ and TNF following re-stimulation with PMA and ionomycin in chronically stimulated T cells with or without N-AC supplementation under normoxic or hypoxic conditions. Experiment was repeated two times with similar results. (b-c) Oxygen consumption rate (OCR) of OT-I T cells chronically co-cultured with B16 melanoma cells with or without anti-PD-L1 antibodies and with or without N-AC supplementation at baseline or in the presence of ATP synthase inhibition (Oligo), uncoupling agents (FCCP), or complex III/IV inhibition (Rot/AA). (d) Production of IFN-γ and TNF following re-stimulation with PMA and ionomycin in chronically stimulated T cells with or without MitoTEMPO or Trolox supplementation as indicated. Experiment was repeated two times with similar results. *P* values were calculated by unpaired, two-sided Student's *t*-test (c). Data are presented as the mean ± s.d. of n=4 biologically independent samples from a representative experiment (b-c). *P<0.05.

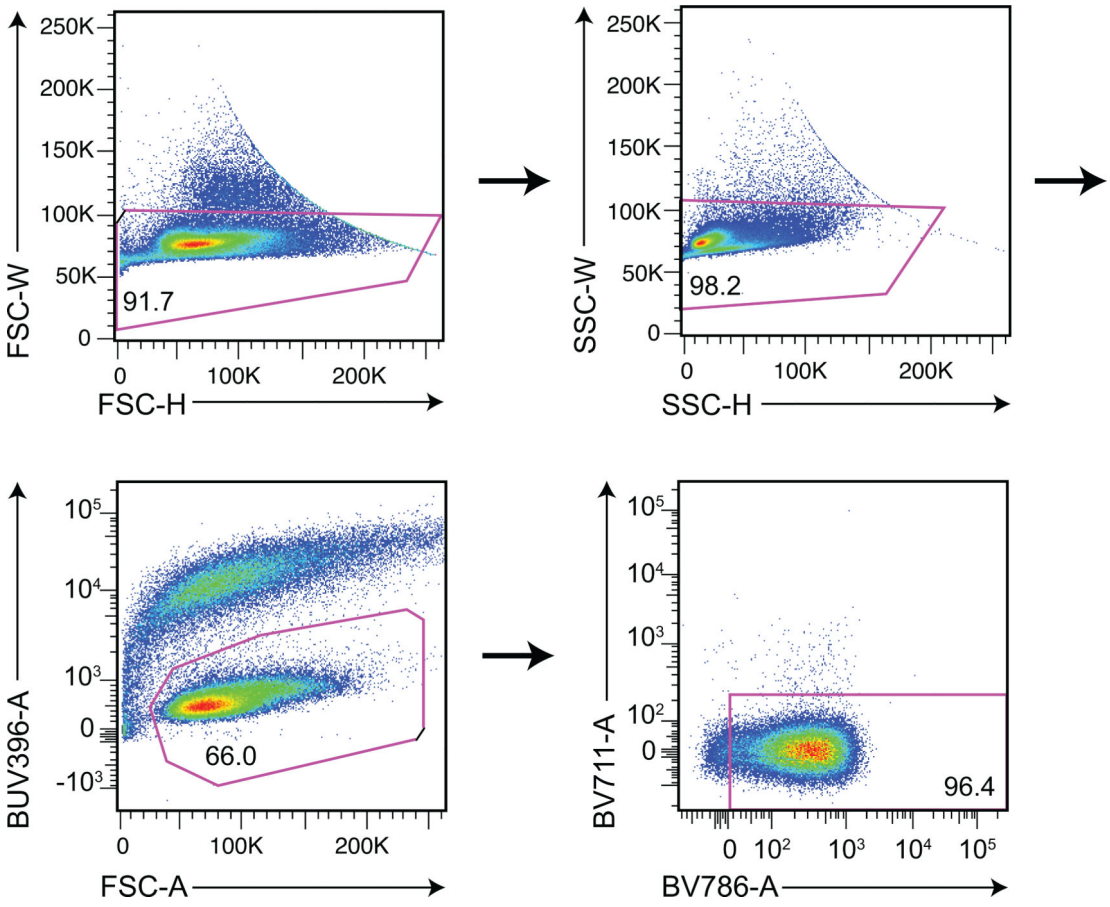

Extended Data Fig. 9. Gating strategy for fluorescence activated cell sorting analysis.

For both polyclonal and OT-I transgenic T cells, gating was perform as shown. First, doublet exclusion was performed on cells gated by FSC-H versus FSC-W. Then, doublet exclusion was performed on cells gated by SSC-H versus SSC-W. Viable cells were identified by FSC-A and Live/Dead Blue exclusion. Finally, CD8 positivity was assessed by fluorescence in the BV-786 channel.

Supplementary Material

Refer to Web version on PubMed Central for supplementary material.

Acknowledgments

We thank members of the Thompson and Finley labs for discussion and critical feedback. S.A.V. is a Senior Fellow with the Parker Institute of Cancer Immunotherapy and is supported by a Burroughs Wellcome Fund Career Award for Medical Scientists. A.T.S. was supported by a Bridge Scholar Award from the Parker Institute for Cancer Immunotherapy and a Career Award for Medical Scientists from the Burroughs Wellcome Fund. This work was additionally supported by the Memorial Sloan Kettering Cancer Center Support Grant P30 CA008748 and R25 Training Grant AI140472-01A1.

Competing Interests

C.B.T. is a founder of Agios Pharmaceuticals and a member of its scientific advisory board. He is also a former member of the Board of Directors and stockholder of Merck and Charles River Laboratories. S.A.V. has received honoraria from Agios Pharmaceuticals and Rheos Pharmaceuticals, is an advisor for Immunai and has consulted for

ADC Therapeutics. A.T.S. and D.K.W. are scientific founders, equity holders and receive consulting fees from Immunai. A.T.S. received funding support from 10x Genomics and Arsenal Biosciences. K.E.Y. is an advisor for Immunai. H.Y.C. is a co-founder of Accent Therapeutics, Boundless Bio, and is a consultant for 10x Genomics, Arsenal Biosciences, and Spring Discovery.

References

1. Hanahan D & Weinberg RA Hallmarks of cancer: the next generation. Cell 144, 646–674 (2011). [PubMed: 21376230]
2. Wherry EJ & Kurachi M Molecular and cellular insights into T cell exhaustion. Nat Rev Immunol 15, 486–499 (2015). [PubMed: 26205583]
3. Ribas A & Wolchok JD Cancer immunotherapy using checkpoint blockade. Science 359, 1350–1355 (2018). [PubMed: 29567705]
4. Siddiqui I et al. Intratumoral Tcf1(+)PD-1(+)CD8(+) T Cells with Stem-like Properties Promote Tumor Control in Response to Vaccination and Checkpoint Blockade Immunotherapy. Immunity 50, 195–211 e110 (2019). [PubMed: 30635237]
5. Kurtulus S et al. Checkpoint Blockade Immunotherapy Induces Dynamic Changes in PD-1(−)CD8(+) Tumor-Infiltrating T Cells. Immunity 50, 181–194 e186 (2019). [PubMed: 30635236]
6. Sade-Feldman M et al. Defining T Cell States Associated with Response to Checkpoint Immunotherapy in Melanoma. Cell 175, 998–1013 e1020 (2018). [PubMed: 30388456]
7. Im SJ et al. Defining CD8+ T cells that provide the proliferative burst after PD-1 therapy. Nature 537, 417–421 (2016). [PubMed: 27501248]
8. Miller BC et al. Subsets of exhausted CD8(+) T cells differentially mediate tumor control and respond to checkpoint blockade. Nat Immunol 20, 326–336 (2019). [PubMed: 30778252]
9. Frauwirth KA et al. The CD28 signaling pathway regulates glucose metabolism. Immunity 16, 769–777 (2002). [PubMed: 12121659]
10. Parry RV et al. CTLA-4 and PD-1 receptors inhibit T-cell activation by distinct mechanisms. Mol Cell Biol 25, 9543–9553 (2005). [PubMed: 16227604]
11. Scharping NE et al. The Tumor Microenvironment Represses T Cell Mitochondrial Biogenesis to Drive Intratumoral T Cell Metabolic Insufficiency and Dysfunction. Immunity 45, 374–388 (2016). [PubMed: 27496732]
12. Siska PJ et al. Mitochondrial dysregulation and glycolytic insufficiency functionally impair CD8 T cells infiltrating human renal cell carcinoma. JCI Insight 2 (2017).
13. Zhang Y et al. Enhancing CD8(+) T Cell Fatty Acid Catabolism within a Metabolically Challenging Tumor Microenvironment Increases the Efficacy of Melanoma Immunotherapy. Cancer Cell 32, 377–391 e379 (2017). [PubMed: 28898698]
14. Macian F et al. Transcriptional mechanisms underlying lymphocyte tolerance. Cell 109, 719–731 (2002). [PubMed: 12086671]
15. Philip M et al. Chromatin states define tumour-specific T cell dysfunction and reprogramming. Nature 545, 452–456 (2017). [PubMed: 28514453]
16. Wherry EJ et al. Molecular signature of CD8+ T cell exhaustion during chronic viral infection. Immunity 27, 670–684 (2007). [PubMed: 17950003]
17. Warburg O On the origin of cancer cells. Science 123, 309–314 (1956). [PubMed: 13298683]
18. Vander Heiden MG, Cantley LC & Thompson CB Understanding the Warburg effect: the metabolic requirements of cell proliferation. Science 324, 1029–1033 (2009). [PubMed: 19460998]
19. Yost KE et al. Clonal replacement of tumor-specific T cells following PD-1 blockade. Nat Med (2019).
20. Yao C et al. Single-cell RNA-seq reveals TOX as a key regulator of CD8(+) T cell persistence in chronic infection. Nat Immunol 20, 890–901 (2019). [PubMed: 31209400]
21. Scott AC et al. TOX is a critical regulator of tumour-specific T cell differentiation. Nature 571, 270–274 (2019). [PubMed: 31207604]

22. Alfei F et al. TOX reinforces the phenotype and longevity of exhausted T cells in chronic viral infection. Nature 571, 265–269 (2019). [PubMed: 31207605]
23. Sullivan LB et al. Supporting Aspartate Biosynthesis Is an Essential Function of Respiration in Proliferating Cells. Cell 162, 552–563 (2015). [PubMed: 26232225]
24. Sena LA et al. Mitochondria are required for antigen-specific T cell activation through reactive oxygen species signaling. Immunity 38, 225–236 (2013). [PubMed: 23415911]
25. Cardenas C et al. Essential regulation of cell bioenergetics by constitutive InsP3 receptor Ca2+ transfer to mitochondria. Cell 142, 270–283 (2010). [PubMed: 20655468]
26. Loffler M, Jockel J, Schuster G & Becker C Dihydroorotat-ubiquinone oxidoreductase links mitochondria in the biosynthesis of pyrimidine nucleotides. Mol Cell Biochem 174, 125–129 (1997). [PubMed: 9309676]
27. Birsoy K et al. An Essential Role of the Mitochondrial Electron Transport Chain in Cell Proliferation Is to Enable Aspartate Synthesis. Cell 162, 540–551 (2015). [PubMed: 26232224]
28. Bauer DE, Hatzivassiliou G, Zhao F, Andreadis C & Thompson CB ATP citrate lyase is an important component of cell growth and transformation. Oncogene 24, 6314–6322 (2005). [PubMed: 16007201]
29. Fraietta JA et al. Determinants of response and resistance to CD19 chimeric antigen receptor (CAR) T cell therapy of chronic lymphocytic leukemia. Nat Med 24, 563–571 (2018). [PubMed: 29713085]
30. Titov DV et al. Complementation of mitochondrial electron transport chain by manipulation of the NAD+/NADH ratio. Science 352, 231–235 (2016). [PubMed: 27124460]
31. Flint DH, Tuminello JF & Emptage MH The inactivation of Fe-S cluster containing hydro-lyases by superoxide. J Biol Chem 268, 22369–22376 (1993). [PubMed: 8226748]
32. Chandel NS et al. Mitochondrial reactive oxygen species trigger hypoxia-induced transcription. Proc Natl Acad Sci U S A 95, 11715–11720 (1998). [PubMed: 9751731]
33. Chang CH et al. Posttranscriptional control of T cell effector function by aerobic glycolysis. Cell 153, 1239–1251 (2013). [PubMed: 23746840]
34. Khan O et al. TOX transcriptionally and epigenetically programs CD8(+) T cell exhaustion. Nature 571, 211–218 (2019). [PubMed: 31207603]
35. Martinez GJ et al. The transcription factor NFAT promotes exhaustion of activated CD8(+) T cells. Immunity 42, 265–278 (2015). [PubMed: 25680272]
36. Bevan MJ, Epstein R & Cohn M The effect of 2-mercaptoethanol on murine mixed lymphocyte cultures. J Exp Med 139, 1025–1030 (1974). [PubMed: 4816300]
37. Mak TW et al. Glutathione Primes T Cell Metabolism for Inflammation. Immunity 46, 675–689 (2017). [PubMed: 28423341]
38. Pauken KE et al. Epigenetic stability of exhausted T cells limits durability of reinvigoration by PD-1 blockade. Science 354, 1160–1165 (2016). [PubMed: 27789795]
39. Sen DR et al. The epigenetic landscape of T cell exhaustion. Science 354, 1165–1169 (2016). [PubMed: 27789799]
40. Shin H et al. A role for the transcriptional repressor Blimp-1 in CD8(+) T cell exhaustion during chronic viral infection. Immunity 31, 309–320 (2009). [PubMed: 19664943]
41. Rutishauser RL et al. Transcriptional repressor Blimp-1 promotes CD8(+) T cell terminal differentiation and represses the acquisition of central memory T cell properties. Immunity 31, 296–308 (2009). [PubMed: 19664941]
42. Gautam S et al. The transcription factor c-Myb regulates CD8(+) T cell stemness and antitumor immunity. Nat Immunol 20, 337–349 (2019). [PubMed: 30778251]
43. Bengsch B et al. Bioenergetic Insufficiencies Due to Metabolic Alterations Regulated by the Inhibitory Receptor PD-1 Are an Early Driver of CD8(+) T Cell Exhaustion. Immunity 45, 358–373 (2016). [PubMed: 27496729]
44. Thommen DS et al. A transcriptionally and functionally distinct PD-1(+) CD8(+) T cell pool with predictive potential in non-small-cell lung cancer treated with PD-1 blockade. Nat Med 24, 994–1004 (2018). [PubMed: 29892065]

45. Schietinger A et al. Tumor-Specific T Cell Dysfunction Is a Dynamic Antigen-Driven Differentiation Program Initiated Early during Tumorigenesis. Immunity 45, 389–401 (2016). [PubMed: 27521269]

46. Taylor A, Rothstein D & Rudd CE Small-Molecule Inhibition of PD-1 Transcription Is an Effective Alternative to Antibody Blockade in Cancer Therapy. Cancer Res 78, 706–717 (2018). [PubMed: 29055015]

47. Ghosh A et al. Donor CD19 CAR T cells exert potent graft-versus-lymphoma activity with diminished graft-versus-host activity. Nat Med 23, 242–249 (2017). [PubMed: 28067900]

48. Pilon-Thomas S, Mackay A, Vohra N & Mule JJ Blockade of programmed death ligand 1 enhances the therapeutic efficacy of combination immunotherapy against melanoma. J Immunol 184, 3442–3449 (2010). [PubMed: 20194714]

49. Liang Y et al. Targeting IFNalpha to tumor by anti-PD-L1 creates feedforward antitumor responses to overcome checkpoint blockade resistance. Nat Commun 9, 4586 (2018). [PubMed: 30389912]

50. Mariathasan S et al. TGFbeta attenuates tumour response to PD-L1 blockade by contributing to exclusion of T cells. Nature 554, 544–548 (2018). [PubMed: 29443960]

Methods-only references

51. Naviaux RK, Costanzi E, Haas M & Verma IM The pCL vector system: rapid production of helper-free, high-titer, recombinant retroviruses. J Virol 70, 5701–5705 (1996). [PubMed: 8764092]

52. Anders S et al. Count-based differential expression analysis of RNA sequencing data using R and Bioconductor. Nature protocols 8, 1765–1786 (2013). [PubMed: 23975260]

53. Subramanian A et al. Gene set enrichment analysis: a knowledge-based approach for interpreting genome-wide expression profiles. Proceedings of the National Academy of Sciences of the United States of America 102, 15545–15550 (2005). [PubMed: 16199517]

54. Butler A, Hoffman P, Smibert P, Papalexi E & Satija R Integrating single-cell transcriptomic data across different conditions, technologies, and species. Nat Biotechnol 36, 411–420 (2018). [PubMed: 29608179]

55. Liberzon A et al. The Molecular Signatures Database (MSigDB) hallmark gene set collection. Cell Syst 1, 417–425 (2015). [PubMed: 26771021]

56. Martindale JL & Holbrook NJ Cellular response to oxidative stress: signaling for suicide and survival. J Cell Physiol 192, 1–15 (2002). [PubMed: 12115731]

57. Schaefer CF et al. PID: the Pathway Interaction Database. Nucleic Acids Res 37, D674–679 (2009). [PubMed: 18832364]

58. van der Windt GJ, Chang CH & Pearce EL Measuring Bioenergetics in T Cells Using a Seahorse Extracellular Flux Analyzer. Curr Protoc Immunol 113, 3 16B 11–13 16B 14 (2016).

59. Vardhana SA et al. Glutamine independence is a selectable feature of pluripotent stem cells. Nat Metab 1, 676–687 (2019). [PubMed: 31511848]

60. Millard P, Letisse F, Sokol S & Portais JC IsoCor: correcting MS data in isotope labeling experiments. Bioinformatics 28, 1294–1296 (2012). [PubMed: 22419781]

61. Schworer S et al. Proline biosynthesis is a vent for TGFbeta-induced mitochondrial redox stress. EMBO J, e103334 (2020). [PubMed: 32134147]

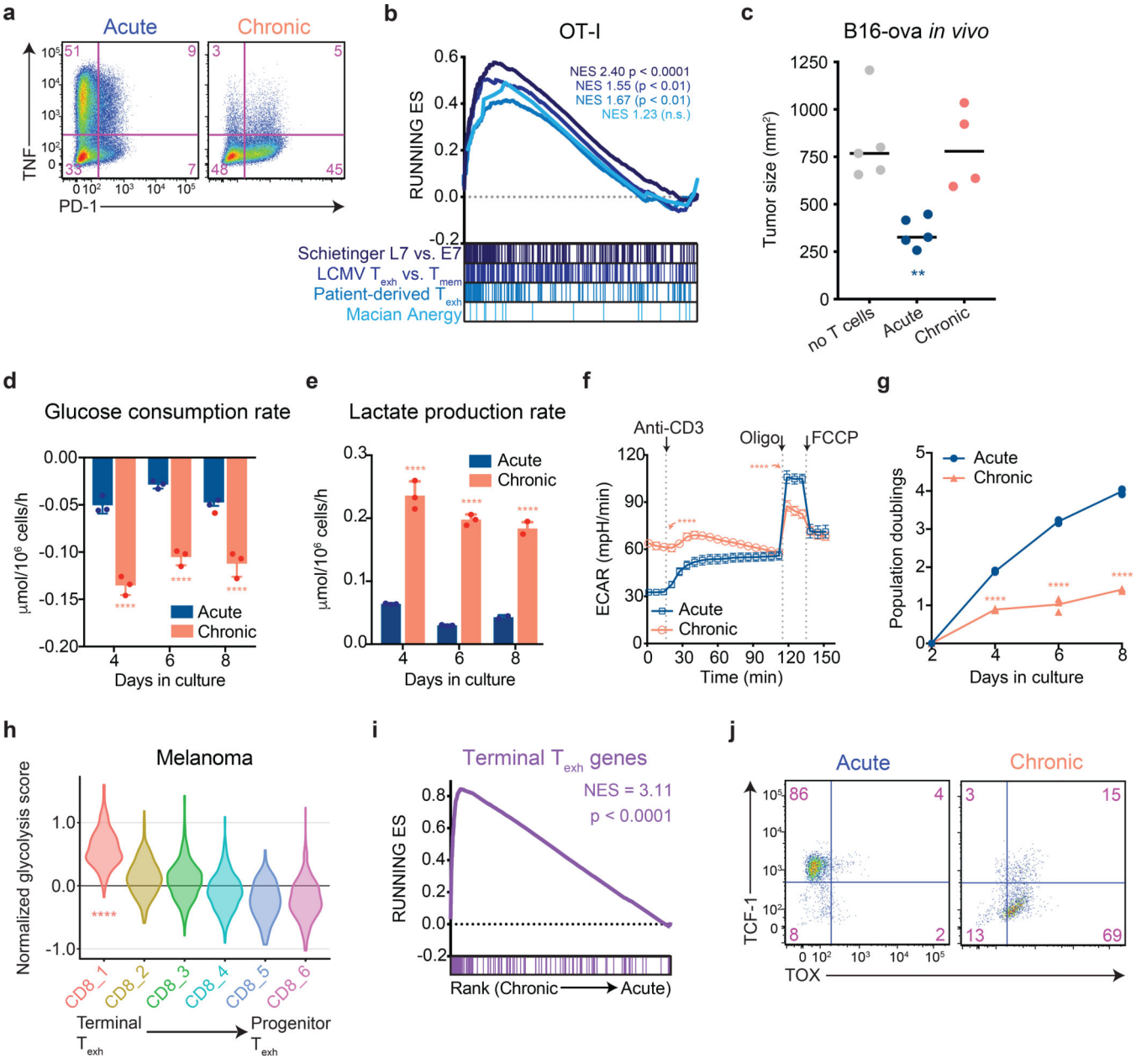

Figure 1. Aerobic glycolysis is a hallmark of terminally exhausted T cells.

All experimental analyses were conducted eight days after initial stimulation unless otherwise specified. (a) PD-1 expression and TNF production by acutely and chronically stimulated T cells upon re-stimulation with PMA and ionomycin. Experiment was repeated three times with similar results. (b) Gene set enrichment plot showing that genes associated with chronically stimulated OT-I T cells *in vitro* are enriched for genes upregulated in exhausted CD8+ T cells but not anergic T cells. (c) Growth of B16-OVA xenografts. Tumor-bearing mice received no T cells or 1 million acutely or chronically stimulated OT-I T cells by adoptive transfer five days after tumor implantation. Tumor size at 14 days post-implantation is shown. (d-e) Median glucose consumed (d) and lactate excreted (e) in acutely and chronically stimulated T cells following initial stimulation. (f) Extracellular

acidification rate (ECAR) of acutely and chronically stimulated polyclonal T cells at baseline, in response to re-stimulation (anti-CD3), or in the presence of ATP synthase inhibition (Oligo) or uncoupling agents (FCCP). (g) Population doublings of acutely and chronically stimulated OT-I T cells following initial stimulation. (h) Normalized expression of glycolytic genes in CD8+ T cell clusters from patients with melanoma treated with immune checkpoint blockade[6]. (i) Gene set enrichment plot showing that chronically stimulated OT-I T cells *in vitro* are enriched for genes upregulated in terminal Texh as compared to progenitor Texh[8]. (j) Flow cytometry plots of acutely and chronically stimulated T cells *in vitro* demonstrating suppression of TCF-1 and upregulation of TOX in chronically stimulated T cells. *P* values were calculated by unpaired, two-sided Student's *t*-test (c-g) relative to acutely stimulated T cells, based on 1,000 permutations by the GSEA algorithm and not adjusted for multiple comparisons (b,i), or Wilcoxon two-sided rank sum test with Benjamini-Hochberg False Discovery Rate (FDR) correction (h). Data are presented as the mean ± s.d. of n=5 (c), n-4 (f) or n=3 (d,e,g) biologically independent samples from a representative experiment. **P<0.01, ****P<0.0001.

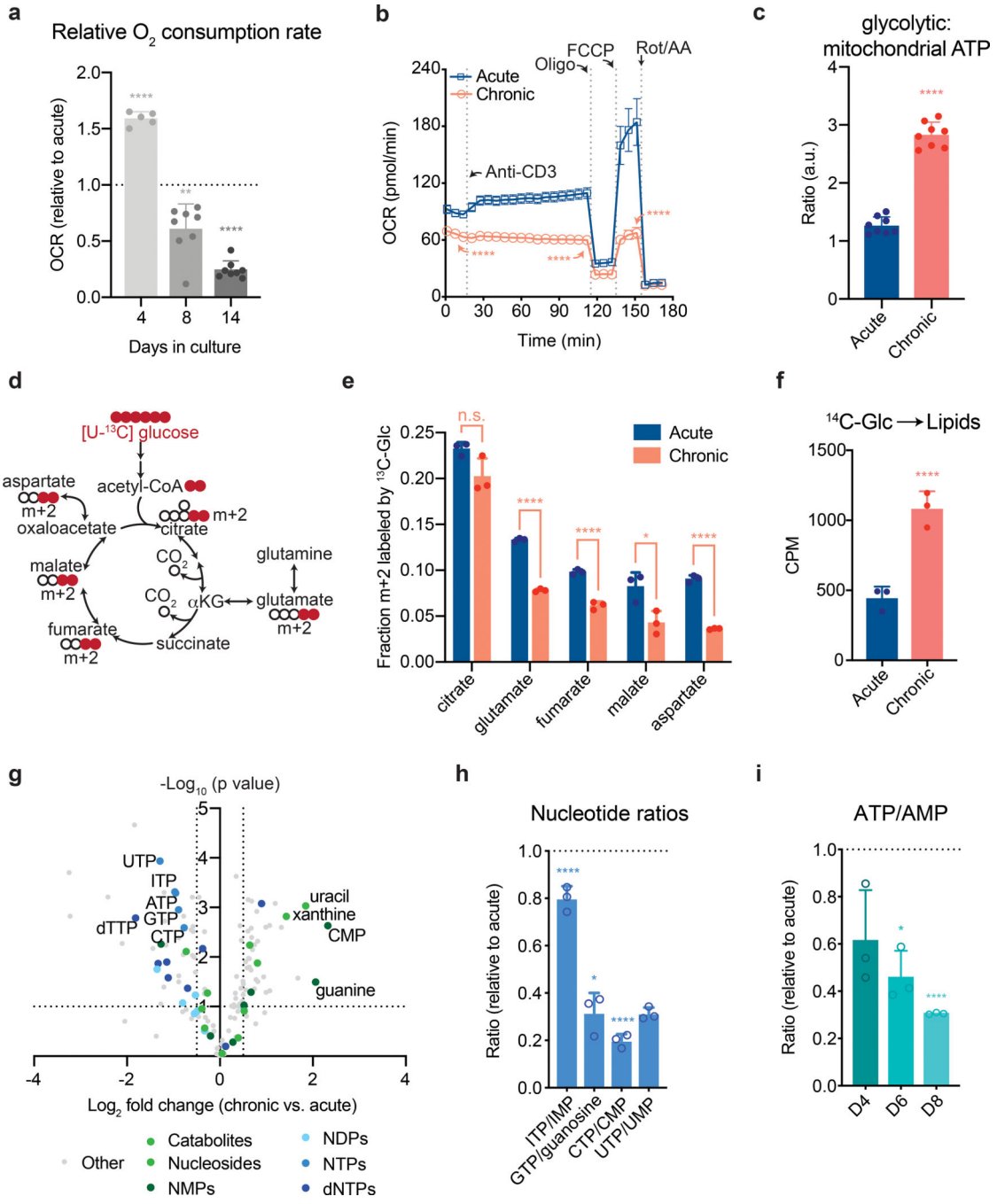

Figure 2. Chronic antigen stimulation induces mitochondrial dysfunction and limits nucleotide biosynthesis.

(a,b) Oxygen consumption rate (OCR) of acutely and chronically stimulated T cells after the indicated days in culture (a) and after 8 days of culture (b) at baseline, in response to re-stimulation (anti-CD3), or in the presence of ATP synthase inhibition (Oligo), uncoupling agents (FCCP), or complex III/IV inhibition (Rot/AA). (c) Ratio of glycolytic to mitochondrial ATP produced by acutely or chronically stimulated cells following re-stimulation with anti-CD3. (d) Schematic depicting how oxidative metabolism of [U-^{13}C] glucose generates metabolites associated with the TCA cycle. Colored circles represent ^{13}C-

labeled carbons. (e) Fractional labeling by [U-^{13}C] glucose of citrate, glutamate, fumarate, malate and aspartate in acutely and chronically stimulated T cells following re-stimulation. (f) Labeling of lipids by [U-^{14}C] after 24 h of culture in acutely and chronically stimulated T cells beginning four days after initial stimulation. (g) Quantification of relative metabolite pool sizes in chronically stimulated T cells compared to acutely stimulated T cells. Colored dots represent nucleotides, nucleosides, and nucleoside catabolites as indicated. Dashed lines represent cutoffs of $p < 0.01$ and $\log_2$ fold change > 0.5. (h-i) Quantification of relative nucleotide ratios of chronically stimulated T cells. Dashed line indicates median ratio in acutely stimulated cells. *P* values were calculated by unpaired, two-sided Student's *t*-test (a-c,e-f) or unpaired, two-sided Student's *t*-test test with Benjamini-Hochberg False Discovery Rate (FDR) correction (g-i). Data are presented as the mean ± s.d. of n=5 (a), n=8 (a,c), n=4 (b), or n=3 (e,f,h,i) biologically independent samples from a representative experiment. *P<0.05, **P<0.01, ****P<0.0001.

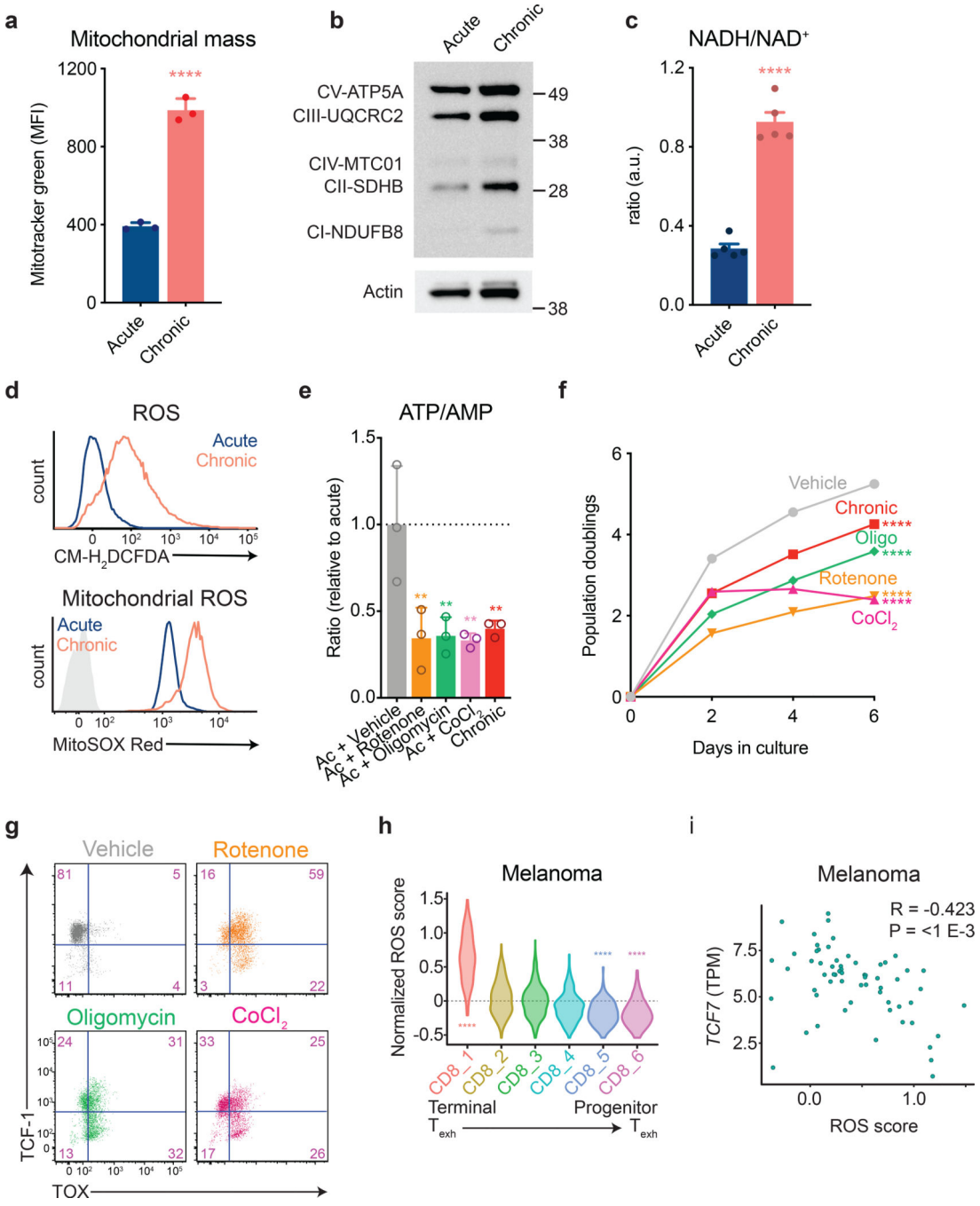

Figure 3. Inhibition of mitochondrial electron transport limits T cell proliferation.

(a) Fluorescence intensity of acutely and chronically stimulated T cells after loading with MitoTracker Green to measure mitochondrial mass. (b) Western blot depicting electron transport chain complex expression in acutely and chronically stimulated T cells. Actin is used as a loading control. Western blot was performed two independent times. Uncropped blot can be found within Source Data. (c) NADH/ NAD+ ratio in acutely and chronically stimulated T cells. Cells were re-stimulated for 30 minutes with anti-CD3 and anti-CD28-coated magnetic beads prior to harvest. Levels were normalized to cell number from

duplicate wells. (d) Fluorescence intensity of acutely and chronically stimulated T cells after loading with CM-H_2DCFDA (above) or MitoSox Red (below). Light-grey-shaded peak represents negative control. (e) ATP/AMP ratios in acutely stimulated T cells cultured with or without the indicated agents following two days of initial stimulation. Dashed line represents median nucleotide ratios in vehicle-treated T cells. (f-g) Population doublings (f) and expression of TCF-1 and TOX (g) of acutely stimulated T cells with or without the addition of the indicated agents following two days of initial stimulation. (h,i) Expression of oxidative stress-related metabolic genes ("ROS score") in tumor-infiltrating CD8+ T cell clusters (h) and correlation of ROS score with *Tcf7* expression in terminally exhausted CD8+ T cell clusters (i) from melanoma patients treated with immune checkpoint inhibitors[6]. *P* values were calculated by unpaired, two-sided Student's t-test (a,c), Wilcoxon two-sided rank sum test with Benjamini-Hochberg False Discovery Rate (FDR) correction (h), one-way ANOVA with Sidak's multiple comparisons post-test (e-f), or based on 1,000 permutations by the GSEA algorithm and not adjusted for multiple comparisons (i). Data are presented as the mean ± s.d. of n=3 (a,e,f) or n=5 (c) biologically independent samples from a representative experiment. **P<0.01, ****P<0.0001.

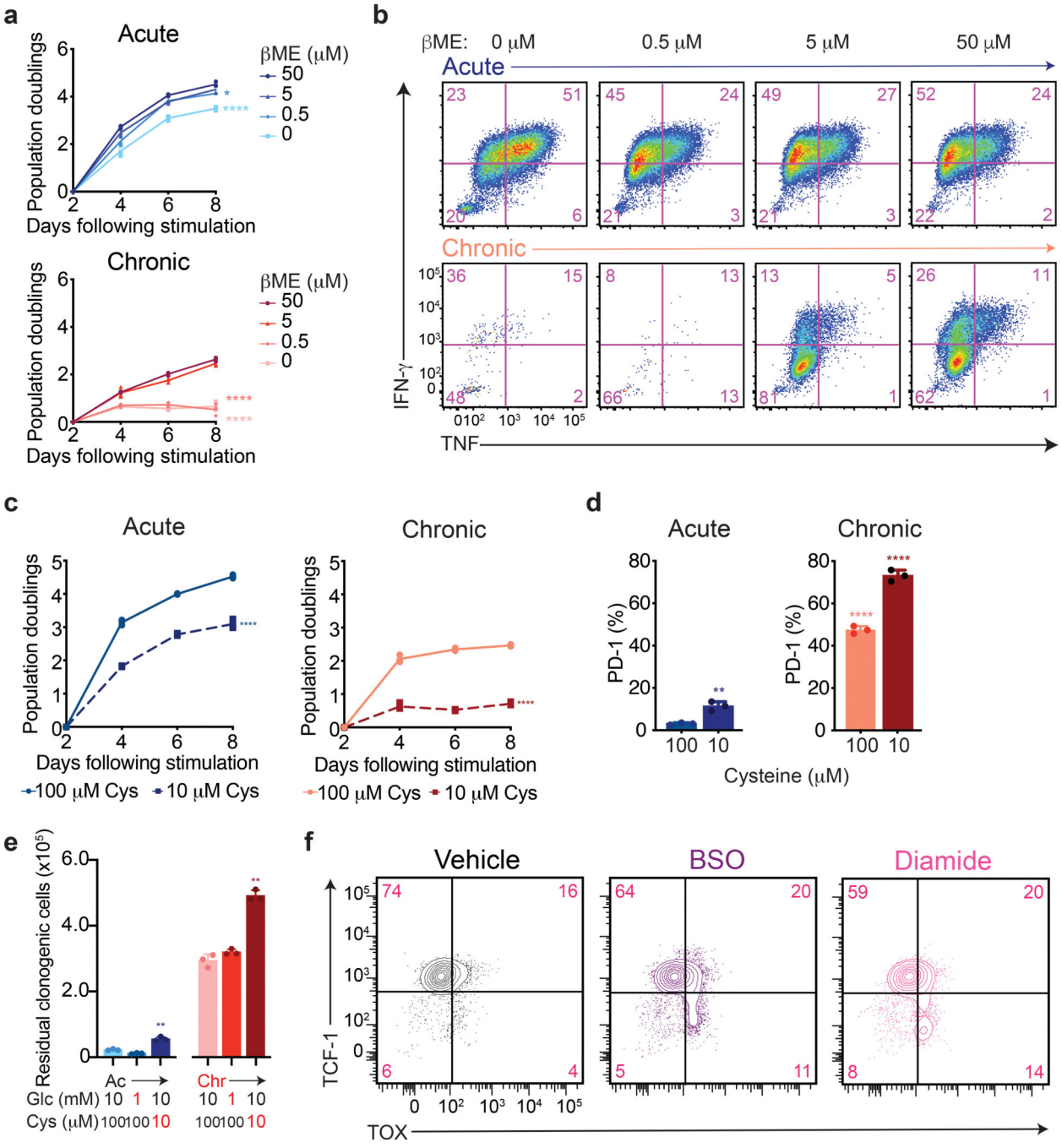

Figure 4. Endogenous antioxidants are required for T cell proliferation.

(a) Effects of β-mercaptoethanol (βME) supplementation on T cell proliferation during acute (upper panel) and chronic (lower panel) stimulation. (b) Effects of βME supplementation on intracellular accumulation of IFN-γ and TNF following re-stimulation with PMA and ionomycin of acutely and chronically stimulated T cells. (c) Effects of extracellular cysteine availability on T cell proliferation during acute (left) and chronic (right) stimulation. (d) Effects of extracellular cysteine availability on PD-1 expression as measured by flow cytometry following re-stimulation with PMA and ionomycin of acutely and chronically

stimulated T cells. (e) Quantification of clonogenic B16 cells following 24 h of co-culture with acutely or chronically stimulated OT-I T cells in media containing nutrients at the indicated concentrations. (f) Expression of TCF-1 and TOX of acutely stimulated T cells with or without the addition of BSO or diamide following two days of initial stimulation. *P* values were calculated by or one-way ANOVA with Sidak's multiple comparisons post-test (a,e) or unpaired, two-sided Student's *t*-test (c-d). Data are presented as the mean ± s.d. of n=3 biologically independent samples from a representative experiment. *P<0.05, **P<0.01, ****P<0.0001.

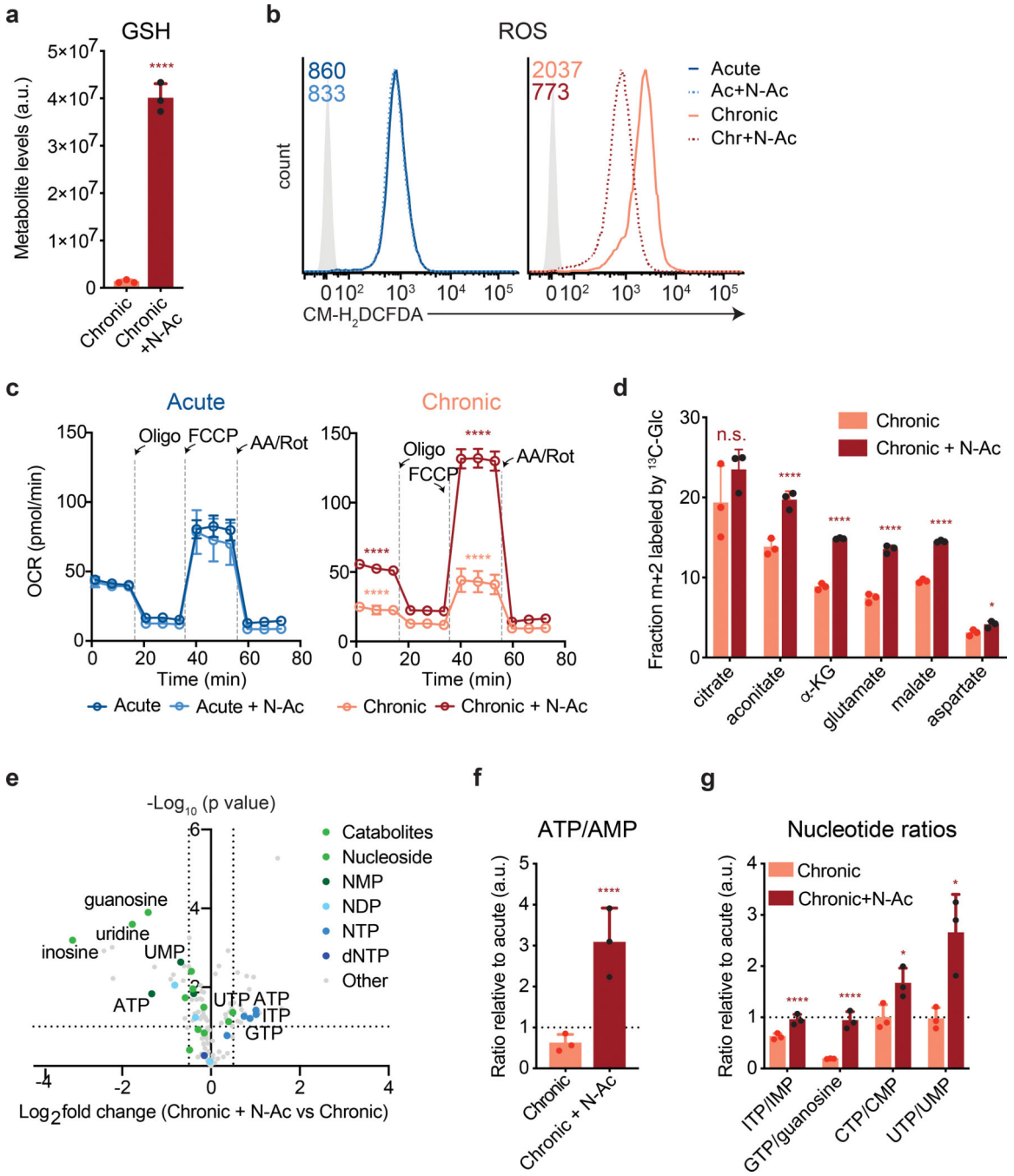

Figure 5. Antioxidants reverse metabolic T cell dysfunction.

(a) Quantification of reduced glutathione pool sizes in chronically stimulated T cells with or without N-AC supplementation as measured by LC-MS. (b) Fluorescence intensity of acutely and chronically stimulated T cells cultured with or without N-AC after loading with CM-H_2DCFDA to measure ROS. Light-grey-shaded peak represents negative control. Geometric mean fluorescence intensity of peaks shown in upper right corner. (c) Oxygen consumption rate (OCR) of T cells cultured with or without N-AC during acute (left) or chronic (right) stimulation at baseline or in the presence of ATP synthase inhibition (Oligo),

uncoupling agents (FCCP), or complex III/IV inhibition (Rot/AA). (d) Fractional labeling by [U-^{13}C] glucose of citrate, aconitate, α-KG, glutamate, malate and aspartate in T cells cultured with or without N-AC during chronic stimulation. (e) Quantification of relative metabolite pool sizes in chronically stimulated T cells with or without N-AC supplementation. Colored dots represent nucleotides, nucleosides, and nucleoside catabolites as indicated. Dashed lines represent cutoffs of $p < 0.01$ and $\log_2$ fold change > 0.5. (f,g) Quantification of relative nucleotide ratios in chronically stimulated T cells with or without N-AC supplementation. Dashed line indicates median ratio in acutely stimulated cells. *P* values were calculated by unpaired, two-sided Student's *t*-test (a,d), unpaired, two-sided Student's *t*-test test with Benjamini-Hochberg False Discovery Rate (FDR) correction (e-g) or one-way ANOVA with Sidak's multiple comparisons post-test relative to acutely stimulated cells (c) or chronically stimulated cells without N-AC (a,c-g). Data are presented as the mean ± s.d. of n=3 (a,d,f,g) or n=4 (c) biologically independent samples from a representative experiment. *P<0.05, ****P<0.0001.

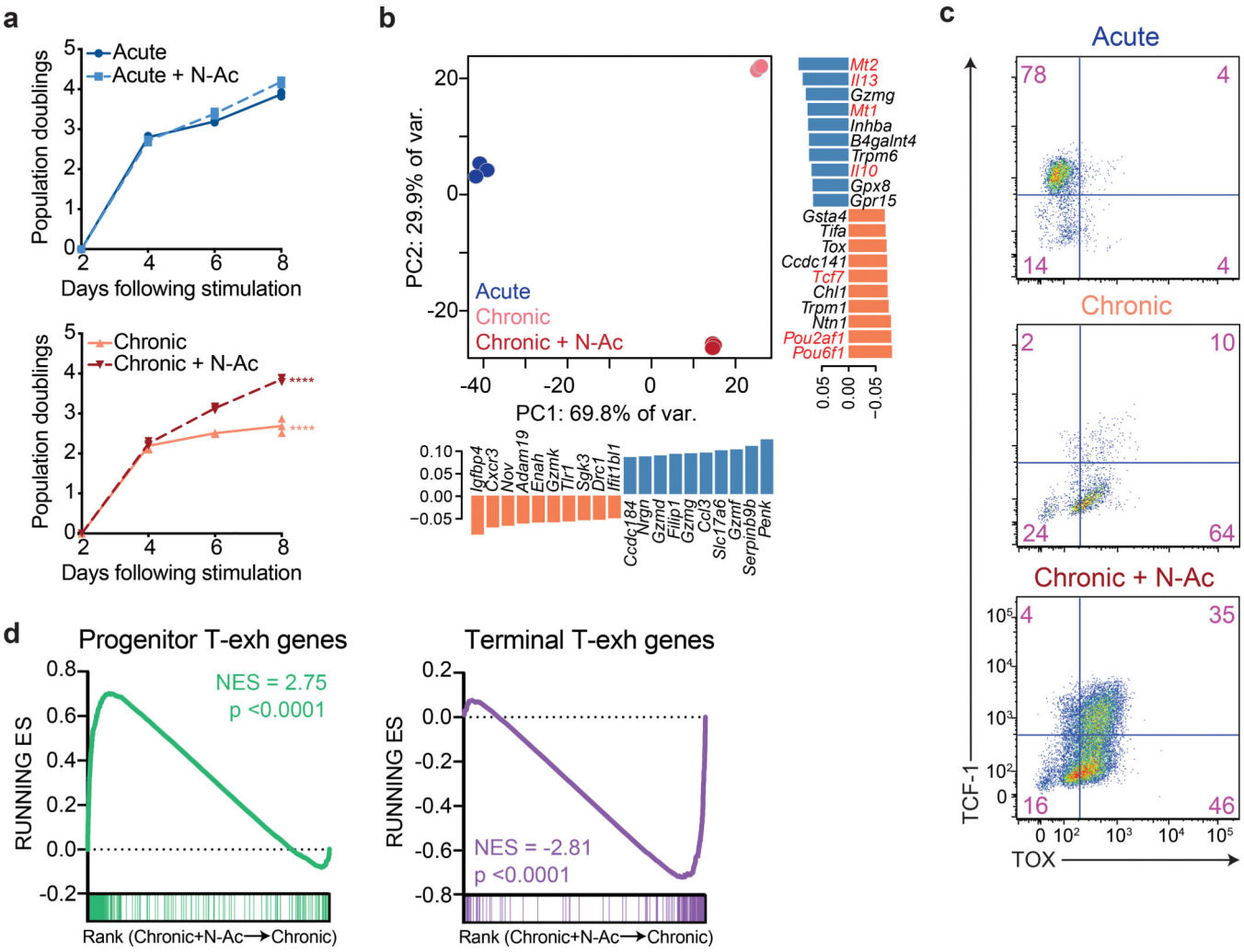

Figure 6. Antioxidants restore the proliferation and self-renewal of chronically stimulated T cells.

(a) Population doublings of acutely (above) and chronically (below) stimulated T cells in media with or without the addition of N-AC as indicated. (b) Principal component analysis of RNA-sequencing of T cells acutely or chronically stimulated with or without N-AC during chronic stimulation. Bar graphs depict genes significantly contributing to variance. (c) Expression of TCF-1 and TOX in acutely or chronically stimulated T cells with or without N-AC during chronic stimulation as indicated. (d) Gene set enrichment plot showing that chronically stimulated T cells cultured in the presence of N-AC are significantly enriched for genes associated with progenitor T_{exh} (left) and significantly depleted of genes associated with terminal T_{exh} (right)[8]. *P* values were calculated by unpaired, two-sided Student's *t*-test (a) or based on 1,000 permutations by the GSEA algorithm and not adjusted for multiple comparisons (d). Data are presented as the mean ± s.d. of n=3 biologically independent samples from a representative experiment. ****P<0.0001.

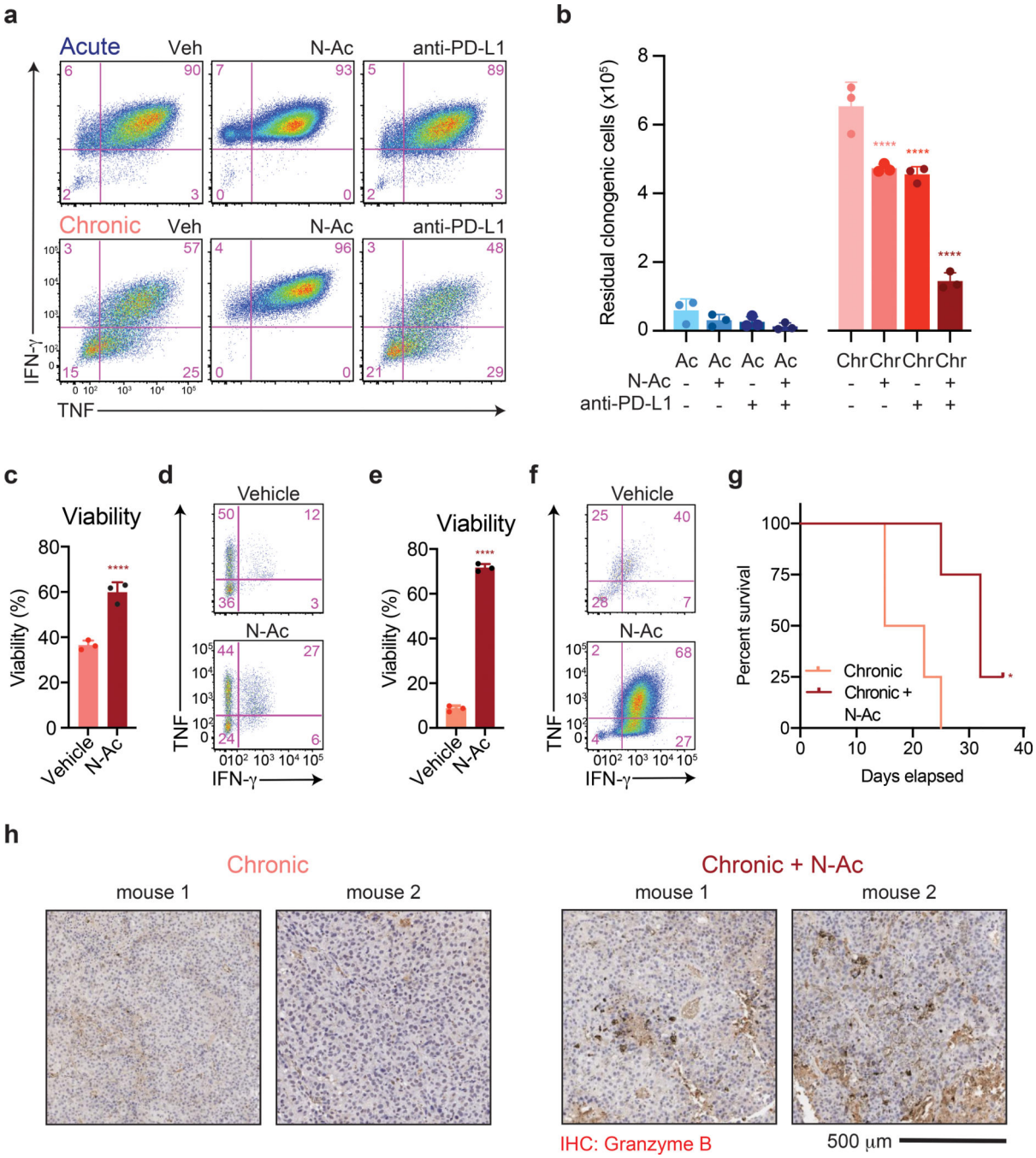

Figure 7. Antioxidants reverse chronic stimulation-driven loss of T cell effector function.

(a) Intracellular accumulation of IFN-γ and TNF following re-stimulation with PMA and ionomycin of T cells following acute or chronic stimulation in the presence or absence of N-AC or anti-PD-L1 as indicated. (b) Quantification of clonogenic B16 cells following 24 h of co-culture with acutely or chronically stimulated OT-I T cells that had been treated with N-AC or anti-PD-L1 throughout the co-culture period. (c-d) Viability (c) and intracellular production of IFN-γ and TNF (d) of CD8+ T cells isolated from EL4 tumors 3 days after re-stimulation in the presence or absence of N-AC. (e-f) Viability (e) and production of IFN-γ

and TNF (f) by CAR-T cells 3 days after re-stimulation in the presence or absence of N-AC. (g) Kaplan-Meier curve showing survival of B16-ova-bearing recipient mice following adoptive transfer of OT-I T cells that had been chronically stimulated in the presence or absence of N-AC. All mice received anti-PD-L1 therapy twice weekly. (h) Immunohistochemistry showing enhanced Granzyme B expression in tumor-infiltrating T cells treated with N-AC. Staining of tumors extracted from two individual mice are shown. *P* values were calculated by one-way ANOVA with Sidak's multiple comparisons post-test (b), unpaired, two-sided Student's *t*-test (c,e) or log-rank (Mantel-Cox) test (g) relative to vehicle-treated cells. Data are presented as the mean ± s.d. of n=3 biologically independent samples or n=5 independent mice (g) from a representative experiment. *P<0.05, ****P<0.0001.